RSC Advances

REVIEW

View Article Online
View Journal | View Issue

Open Access Article. Published on 04 June 2020. Downloaded on 11/7/2025 11:42:49 AM.
This article is licensed under a Creative Commons Attribution-NonCommercial 3.0 Unported Licence.

Check for updates

Cite this: *RSC Adv.*, 2020, **10**, 21561

Developments and applications of nanomaterial-based carbon paste electrodes

Somayeh Tajik,[a] Hadi Beitollahi,*[b] Fariba Garkani Nejad,[b] Mohadeseh Safaei,[b] Kaiqiang Zhang,[c] Quyet Van Le,*[d] Rajender S. Varma,[e] Ho Won Jang[f] and Mohammadreza Shokouhimehr*[f]

Received 24th April 2020
Accepted 27th May 2020

DOI: 10.1039/d0ra03672b

rsc.li/rsc-advances

This review summarizes the progress that has been made in the past ten years in the field of electrochemical sensing using nanomaterial-based carbon paste electrodes. Following an introduction into the field, a first large section covers sensors for biological species and pharmaceutical compounds (with subsections on sensors for antioxidants, catecholamines and amino acids). The next section covers sensors for environmental pollutants (with subsections on sensors for pesticides and heavy metal ions). Several tables are presented that give an overview on the wealth of methods (differential pulse voltammetry, square wave voltammetry, amperometry, *etc.*) and different nanomaterials available. A concluding section summarizes the status, addresses future challenges, and gives an outlook on potential trends.

Introduction

Over the last few decades, some conventional analytical methods like gas chromatography/mass spectrometry (GC/MS), atomic absorption spectroscopy, high-performance liquid chromatography (HPLC), spectrofluorimetry, capillary electrophoresis, flow injection chemiluminescence, *etc.* have been used to detect important compounds. However, these analytical techniques are time-consuming, expensive, require lots of expertise to be carried out and are not easy to deploy in the field due to their bulky equipment. Instead, in the analysis of different important species, electrochemical methods have been developed due to their simplicity, rapidity, low cost of equipment, high sensitivity and accurate analytical tools.[1–13]

In general, electrochemical methods are based on the transformation of chemical information into an analytical and electrochemically measurable signal. In recent years, scientists pay attention to new electrode materials characterized by broader potential window, higher signal-to-noise ratio, mechanical stability enabling their application in flowing systems, and resistance toward passivation. The last requirement is especially important because electrode fouling is probably the biggest obstacle to more frequent applications of electroanalytical methods in environmental analysis. A short time before Professor Jaroslav Heyrovsky was awarded the Nobel Prize for chemistry in 1958 and his polarographic approach becoming a worldwide success, Adams presented a novel type of electrode.[14–16] The suitable substance for this sensor was created by a concoction of carbon powder with a liquid non-electroactive binder which was simply called carbon paste. The structure of the carbon was identical to DME, *i.e.* originating from a reservoir with carbon power suspension within a liquid which is connected to a capillary that allows one to acquire sporadically renewable carbon electrode droplets.[17,18]

Carbon is useful electrode material, particularly where high current densities; wide potential range and long term stability were desired. In fact, carbon and its derivatives, as the high performance material, occupy a special place in electrochemistry.[19–23]

Carbon paste electrodes (CPEs) have attracted attention as electrodes mainly due to their advantages such as chemical inertness, robustness, renewability, stable response, low ohmic resistance, no need for internal solution and suitability for a variety of sensing and detection applications.[24–26] Moreover, CPEs belong to nontoxic and environmentally friendly electrodes. In their case, problems with passivation are simply eliminated by a simple and quick renewal of their surface. However, traditional CPEs suffer from numerous shortcomings for electro-chemical detection, including lower sensitivity and reproducibility, slower kinetic of electron transfer, lower stability on a wide range

[a]*Research Center for Tropical and Infectious Diseases, Kerman University of Medical Sciences, Kerman, 7616913555, Iran*

[b]*Environment Department, Institute of Science and High Technology and Environmental Sciences, Graduate University of Advanced Technology, Kerman, Iran. E-mail: h.beitollahi@yahoo.com*

[c]*Jiangsu Key Laboratory of Advanced Organic Materials, Key Laboratory of Mesoscopic Chemistry of MOE, School of Chemistry and Chemical Engineering, Nanjing University, Nanjing, Jiangsu 210023, China*

[d]*Institute of Research and Development, Duy Tan University, Da Nang 550000, Vietnam. E-mail: Levanquyet@dtu.edu.vn*

[e]*Regional Centre of Advanced Technologies and Materials, Department of Physical Chemistry, Faculty of Science, Palacky University, Šlechtitelů 27, 783 71 Olomouc, Czech Republic*

[f]*Department of Materials Science and Engineering, Research Institute of Advanced Materials, Seoul National University, Seoul 08826, Republic of Korea. E-mail: mrsh2@snu.ac.kr*

Open Access Article. Published on 04 June 2020. Downloaded on 11/7/2025 11:42:49 AM.
This article is licensed under a Creative Commons Attribution-NonCommercial 3.0 Unported Licence.

of solution compositions, and the need for greater over-potential for electro-catalytic process. These problems may be resolved *via* modifying the electrodes.[27–33] Notably, the chemically modified electrodes augment the transfer rate of electron by declining over-voltage. Nanomaterials based chemical modified electrode's have been the spotlight because of their increased sensitivity, the amplified response signals, and more acceptable reproducibility.[34–41]

This report concerns the progressions in nanomaterials-based CPEs in electro-analysis. Several published papers entailing substantial breakthroughs have been covered in the field of CPEs. This report provides a summary of the current literature and does not intend to address some reported advancements. It is focused on original designs, materials and methods concerning CPEs in addition to implementations in electro-analysis.

Fabrication of CPEs

Methods for preparation of CPEs have been described in many reviews and books,[42–47] which we will briefly describe below. Soft carbon pastes are conventionally packed into adequate electrode bodies. A holder for carbon pastes can be realized as a well drilled into a short Teflon rod,[48] a glass tube or a polyethylene syringe filled with a paste, which is electrically contacted *via* a conducting wire.[49,50] In general tests, CPE holders did not exhibit significant changes regarding design and functionality.[51–54] The diameter of the end hole shaping the suitable carbon paste surface is selected in the 2 mm to 10 mm range for typical CPEs, and is adequate for most electrochemical measurements.[55–61] The construction alternatives for the CPEs mentioned above are a vital characteristic of carbon pastes which entails easy and prompt surface renewal and if required, large portions of the paste may be removed or renewed. In practice, prompt renewal of the surface may be done by wiping the paste using wet filter paper. When cautiously conducted, this process enables surface reproducibility that is almost comparable to that obtained using tedious methods such as using a paper pad to polish the electrode surface. More appealing CPEs designs are typically seen with electrochemical detectors, carbon paste-based flow cells, coulometric, potentiometric and amperometric sensors or sensing apparatus for specific vivo based measurements.[62–68] As an example, electrochemical assessments regarding electrode response modulation may be conducted using sporadically renewed carbon paste *via* a specific cell supplied with doubled carbon paste filling. As well as others, this design entailing intimate surface renewal is highly influential on analyzing biological and organic substances with readily poisoned electrode surface either with electrode reaction products or matrix constituents.[69–71]

Physico-chemical and electrochemical properties of CPE

The disposition and behavior of typical carbon pastes may be displayed using the physico-chemical properties listed below:

- Instability in non-aqueous solution (dissolution).
- Low ohmic resistance (highly conductive).
- Lipophilicity (hydrophobicity).
- Heterogeneity (composite characteristic).
- Ageing impact (limited life).

Such characteristics are closely linked to a particular carbon paste microstructure. In the recent past, unprecedented changes of carbon paste microstructure real images have been introduced on the basis of scanning electron and optical microscopic findings.[72–76] These images have proved the findings of prior researches that carbon pastes denote concoctions with unconsolidated formation where graphite particles are essentially covered *via* an extremely thin binder film. Nonetheless, the individual graphite particles evidently have physical contact underneath the binder layer and can be the reason for an extremely low ohmic resistance of the majority of carbon pastes (which vary in ohms, max. in tens of ohms). Other perceptions of their suitable conductivity may be accredited to the tunnel effect that is similar to that of semiconductors.[77–81]

The hydrophobicity is evidently the most commonly witnessed characteristic of carbon paste-based electrodes. The lipophilic property of chemically modified carbon paste electrodes (CMCPEs) and CPEs cause particular reaction kinetics regarding numerous organic redox systems' electrode reactions. In addition to moderated rates, they exhibit a repelling impact of pasting liquid impeding the accessibility of hydrophilic substances that are involved within electrode reactions toward carbon paste surfaces. The graphite quality also affects reaction kinetics which is similar to carbon solid electrodes. Ultimately, the carbon to pasting liquid ratio may also be a significant factor in this regard. A detailed perception of such phenomena along with relevant consequences, is not within the scope of this paper and may be referred to in a paper by Adams *et al.* or in more recent papers. Carbon paste mixtures may be subjected to substantial changes in time *i.e.* the ageing of CPEs. Such property is rarely referred to in the literature and has characteristics regarding carbon pastes consisting of more volatile binders, namely organo phosphates. This unfavorable activity has proved rational assumptions that carbon pastes ageing is accredited only to the binder characteristics. No similar roles of graphite have been reported up to today.[82–89]

Modified CPE

The basis of the adjusted carbon pastes is typically a concoction of a non-electrolytic binder and powdered graphite. Another component within the concoction is a modifier. The modifying agent is typically a substance but more components may be used to form the pastes where regarding the carbon paste-based biosensors, also contain enzymes (or relevant carrier) in addition to an adequate mediator or CMCPEs supplied with a concoction of two modifiers. The quantity of modifiers is dependent on the property of the modifying agent and its competency in creating adequate active sites within modified paste (for example, functional groups, debilitated at electrode surface or extractant molecules in the bulk). Generally, the predominant reason in modifying electrodes is to acquire

Open Access Article. Published on 04 June 2020. Downloaded on 11/7/2025 11:42:49 AM.
This article is licensed under a Creative Commons Attribution-NonCommercial 3.0 Unported Licence.

qualitative new sensors with favorable, pre-defined characteristics. In this regard, carbon pastes are without a doubt, one of the most advantageous substances used to prepare modified electrodes.[90–94] Contrary to comparatively complex adjustments of solid substrates, CMCPEs preparation is straightforward, usually, *via* different alternative processes. A modifier may be disintegrated directly within the binder or mechanically amalgamated within the paste amidst homogenization. Also, it is possible to soak graphite particles using a modifier solution and impregnate carbon powder upon evaporating the solvent. Subsequently, ready-prepared pastes may be adjusted *in situ*. Although direct adjustments clearly present specific sensors for a single purpose implementation, considerate *in situ* methods provide an option to apply the same carbon paste for frequent modifications using various agents.[95–97] Four possible modifier functions are categorized by Kalcher as follows:

- Adjustment of the CPE surface properties.
- Acting in catalytic electrochemical reactions.
- Electrode reactions mediation by means of immobilized molecules or relevant fragments.
- Preferential entrapment of favorable species *e.g.* preconcentration in stripping analysis.

The consideration of such potential combined with the mentioned carbon paste flexibility has entailed numerous diverse substances used for CMCPEs preparation which have grown in geometric order in the past decade. Amidst the currently used modifiers, there are single compounds, specific inorganic substances and matrices, sophisticated chemical agents and living organisms. Conventional modifiers are categorized into different groups.[98–107]

Nanomaterials-based CPEs

Nanotechnology refers broadly to a field of applied science and technology whose unifying theme is the control of matter on the atomic or molecular level in scales 1 to 100 nanometers, and the fabrication of devices within that size range.

The key point to obtain a good and reliable electrochemical sensor lies on the kind of material that constitutes the detection platform. In this field, nanomaterials have brought many advantages. On the development of new electrochemical transducing platforms beside their use as electrochemical labels or tags for signal enhancement with interest for sensing technologies.[108,109] The unique electronic, chemical and mechanical properties of nanomaterials (*i.e.* carbon nanotubes, graphene, metal oxide nanoparticles, metal nanoparticles and *etc.*) make them extremely attractive for electrochemical sensors in comparison to conventional materials.[110–112] Sensing using nanostructured materials takes advantage of the increased electrode surface area, increased mass-transport rate, and fast electron transfer compared to electrodes based on bulk materials between other factors.[113] The synergy between electrochemical sensors technology and nanomaterials is expecting to bring interesting advantages in the field of electroactive compounds detection and is therefore a promising area of research and development. In this review, the aim is to give an overview on the latest trends in the development of electrochemical sensing strategies using nanomaterials during the last 10 years although their relatively longer history.

Electroanalytical applications of modified CPEs

Biological species and pharmaceuticals compounds

Antioxidants. Oxidative stress produces damage to lipids, proteins, deoxyribonucleic acid (DNA) and small cellular molecules impeding normal cell functioning. These biochemical alterations are implicated in a growing list of human diseases, such as cardiovascular diseases, aging, Parkinson's disease, Alzheimer's disease, diabetes and cancer.[114–116] Antioxidants are compounds that inhibit or delay the oxidation process by blocking the initiation or propagation of oxidizing chain reactions. They may function as free radical scavengers, complexers of pro-oxidant metals, reducing agents and quenchers of singlet oxygen.[117–120]

Karimi Maleh *et al.* explain the progression, electrochemical characterization and use of modified *N*-(4-hydroxyphenyl)-3,5-dinitrobenzamide-FePt/carbon nanotube (NHPDA/FePt/CNT) CPE to electro-catalytically ascertain glutathione (GSH) with the existence of piroxicam (PXM). The adjust electrode displayed a competent and continuous electron mediation activity along with favorably separated oxidation peaks of PXM and GSH. Peak currents depended linearly on GSH concentrations within the 0.004–340 μM range with 1.0 nM detection limit. The sensitivity of the modified electrode towards the oxidation of GSH in the absence and presence of PXM were found to be 0.168 $\pm$ 0.023 and 0.167 $\pm$ 0.043 μA μM^{-1}, respectively. This modified electrode was implemented with success to ascertain analytes within real specimens.[121]

Rezaei *et al.* produced a trichloro(terpyridine)ruthenium(III)/multi-wall carbon nanotubes modified paste electrode (TChPRu-MWCNT) and applied it as electro-catalyst to oxidize GSH. The GSH oxidation peak potential at adjusted electrode surface was 270 mV which was 330 mV less than that of conventional CPEs under identical circumstances. There was a linear increase of electro-catalytic currents with GSH concentration across the 0.6–56.8 μM concentration range with a sensitivity of 0.1068 μA μM^{-1}. The relevant GSH detection limit was 0.3 μM. In order to ascertain the GSH of real specimens, namely hemolysed erythrocyte and urine, the electrochemical sensor was studied.[122]

Tahernejad *et al.* conducted a study where they evaluated the impact of admixing MgO, single-wall carbon nanotube (SWCNT) and 2-chloro-*N*′-[1-(2,5-dihydroxyphenyl)methylidene] aniline (2-CDHPMA) within a carbon paste matrix, taking the role of a voltammetric sensor to analyze GSH. Using the square wave voltammetric method (SWV), a linear dynamic range of 0.05–700.0 μM with limit of detection (LOD) ~10 $\pm$ 0.3 nM was set to analyze GSH. The voltammetric sensor displayed 0.0824 μA μM^{-1} sensitivity.[123]

Beitollah *et al.*, synthesized Ag–ZnO nanoplates and 2-chlorobenzoyl ferrocene (2CBF) and applied it to create an altered CPE. GSH surface oxidization of the altered electrode

Open Access Article. Published on 04 June 2020. Downloaded on 11/7/2025 11:42:49 AM.
This article is licensed under a Creative Commons Attribution-NonCommercial 3.0 Unported Licence.

was examined. At optimal conditions, the GSH SWV peak current was linearly increased with GSH concentrations at 5.0×10^{-8} to 2.0×10^{-4} M range with sensitivity of 0.659 μA μM^{-1} and 20.0 nM detection limit acquired for GSH. The produced altered electrode displays a favorable resolution among the GSH and tryptophan (TRP) voltammetric peaks making it appropriate to detect GSH with the existence of TRP within real specimens.[124]

A CPE altered using ethynylferrocene (EF) and NiO/MWCNT nanocomposite was implemented by Roodbari Shahmiri *et al.* to oxidize GSH and acetaminophen (AC). There was a linear increase in terms of SWV peak current at 0.01–200 μM concentration range and 0.006 μM detection limit, correspondingly. The sensitivity of the modified electrode toward the oxidation of GSH in the absence and presence of AC were found to be 1.056 ± 0.041 and 1.179 ± 0.081 μA μM^{-1}, respectively. The altered electrode was applied with favorable results to determine the analytes within real specimens.[125]

Abellan-Llobregat produced an electrochemical sensor on the basis of 4-aminobenzoic acid (4ABA) adjusted herringbone carbon nanotubes (hCNTs) to determine ascorbic acid (AA) within physiological solutions. At a 0.65 μM detection limit, favorable results were achieved for AA. The sensitivity of the electrochemical sensor toward AA was found to be (9.0 ± 0.4) A g^{-1} mM^{-1}.[126]

Tashkourian and Nami-Ana produced an altered CPE supplied with SiO_2 nanoparticles to ascertain gallic acid (GA) Within the 8.0×10^{-7} to 1.0×10^{-4} M concentration range, the altered CPE exhibited sensitivity towards GA which was determined using voltammetric studies. The LOD and sensitivity were calculated as 2.5×10^{-7} M and 1790.7 (μA mM^{-1}), correspondingly. Lastly, the suggested electrochemical sensor was applied with favorable results to ascertain GA within tea and orange juice specimens.[127]

Shahamirifard *et al.* altered a CPE using a nanocomposite consisting of zirconia nanoparticles (ZrO_2NPs), choline chloride (ChCl) and gold nanoparticles (AuNPs) as an electrochemical sensor to concurrently electro-oxidize GA and uric acid (UA). This sensor exhibited a linear reaction within the 0.22–55 μM range and 25 nM low LOD under optimal conditions for GA, correspondingly. The adjusted electrode displayed 1.2943 μA M^{-1} sensitivity. The adjusted electrode was implemented with favorable results to independently ascertain GA in fruit juice and green tea in addition to concurrently ascertaining UA and GA within urine specimens.[128]

Tashkourian *et al.* fabricated an adjusted CPE by using TiO_2 nanoparticles in the carbon paste matrix. The electrochemical activity of GA was also examined. At optimal conditions, 2.5×10^{-6} to 1.5×10^{-4} M linear dynamic range with 9.4×10^{-7} M LOD was acquired for GA. The modified electrode showed a very good sensitivity of 999.4 A mM^{-1}. This modified electrode was applied with satisfactory results within real specimen analysis.[129]

Valizadeh *et al.* described an electrochemical sensor on the basis of metal–organic framework composite of type MIL-101(Fe) adjusted CPE to determine citric acid (CA). This sensor exhibited beneficial analytical characteristics to determine CA at 4.0 μM detection limit, 5.0–100 μM wide linear range and −0.67 μA μM^{-1} cm^{-2} high sensitivity.[130]

Catecholamines. Catecholamines consists of a nucleus catechol group which is categorized as a benzene group containing two adjoining hydroxyl groups in addition to an ethylamine side chain containing a single amine group which can

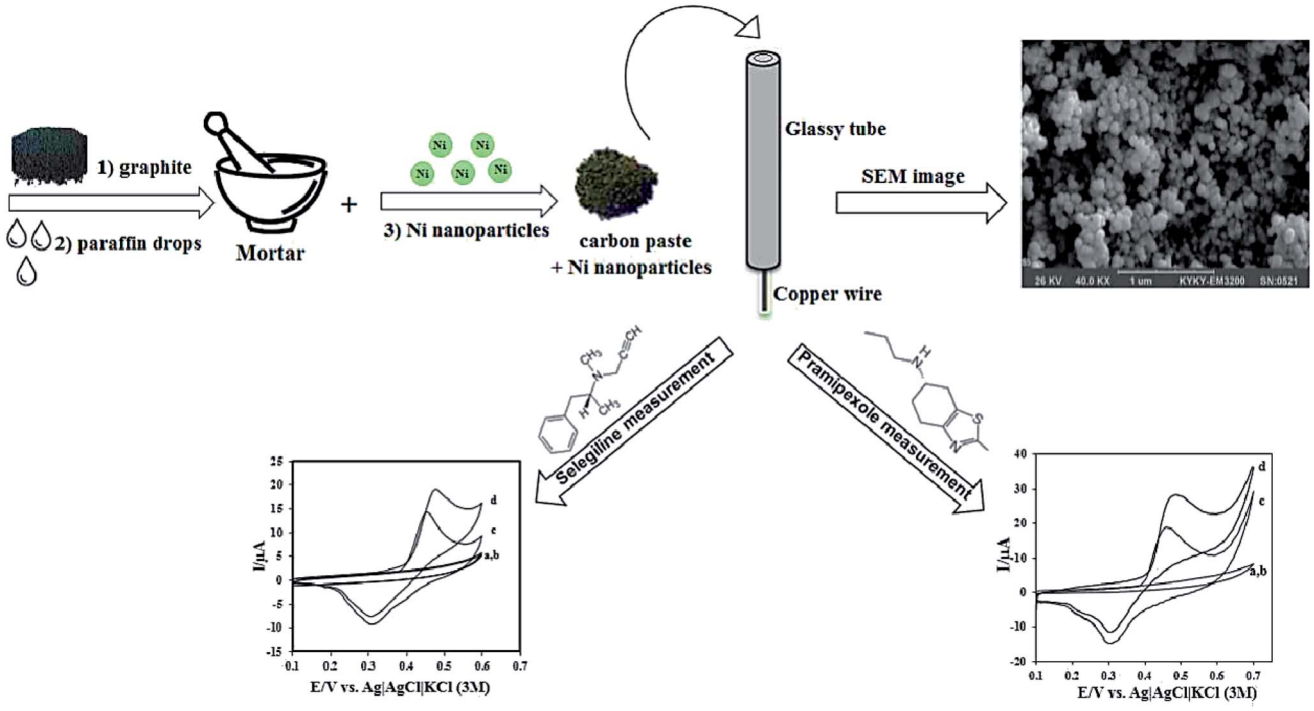

Fig. 1 Schematic illustration of the stepwise fabrication process nickel nanoparticles modified CPE. Reprinted with permission from ref. 137 Copyright (2016) Royal Society of Chemistry.

Open Access Article. Published on 04 June 2020. Downloaded on 11/7/2025 11:42:49 AM. This article is licensed under a Creative Commons Attribution-NonCommercial 3.0 Unported Licence.

entail supplementary alternatives. The prevalent catecholamines inside the brain are epinephrine (EP), norepinephrine (NE) and dopamine (DA). Catecholamines are synthesized within nerves upon release in cell bodies and at terminals. The conversion of its substrates tyrosine (Tyr) and molecular oxygen to 3,4-dihydroxy-L-phenylalanine is conducted by tyrosine hydroxylase (tyrosine 3-monooxygenase). This is the most prominent enzyme within catecholamine synthesis and is the primary and rate restricting stage regarding DA, NE and EP synthesis. Catecholamines are present at low micromolar concentrations inside the brain concerning amino acid neurotransmitters, namely γ-aminobutyric acid and glutamate.[131–136]

Ojani *et al.* conducted a study on dopaminergic drugs' electrocatalytic oxidation, namely selegiline (SEL) and pramipexole (PX) *via* nickel nanoparticles altered CPE (Fig. 1). The associated electrocatalytic oxidation peaks linearly depended on relevant concentrations. A LOD and correlation coefficient of 4.0×10^{-6} M and 0.9951 was acquired for SEL and 4.5×10^{-8} M and 0.9948 for PX. The sensitivity values determined at 4.84×10^{-2} μA μM^{-1} and 4.46×10^{-2} μA μM^{-1} for SEL and PX, respectively. The sensor displayed favorable sensitivity and selectivity and was applied to clinically examine SEL and PX with satisfactory results.[137]

Mazloum Ardakani *et al.* conducted a study to implement a CPE adjusted by *N*,*N*′-(2,3-dihydroxybenzylidene)-1,4-phenylenediamine (DHBPD) and TiO_2 nanoparticles to ascertain DA. They concluded that under optimal conditions using the CV approach, there was a significant drop of overpotential for DA oxidation at the adjusted electrode. DPV displayed 0.08 to 20.0 μM linear dynamic range and 3.14×10^{-8} M LOD concerning DA. The adjusted electrode showed sensitivity 6.525 μA μM^{-1}. This adjusted electrode was applied to ascertain DA in DA injections *via* the standard addition method.[138]

Ye *et al.* produced a CPE that was modified using graphene oxide (GO)/lanthanum (La) complexes to selectively ascertain of DA *via* differential pulse voltammetry (DPV) and cyclic voltammetry (CV). Under optimum condition, the reaction of the adjusted electrode to determine DA was linear within the 0.01–400.0 μM range. The relevant LOD was 0.32 nM. The modified electrode showed two sensitivity of −170.7 μA μM^{-1}. This reformed electrode was used to detect DA within serum and real urine specimens *via* the standard addition method.[139]

Beitollahi *et al.* reported a CdTe quantum dots (QD) reformed CPE to examine DA and UA electro-oxidation including associated mixtures *via* electrochemical approaches. A significantly sensitive and concurrent ascertaining of UA and DA was examined at the reformed electrode using SWV. The SWV peak current for DA exhibited linear enhancement at 7.5×10^{-8} to 6.0×10^{-4} M concentration range. The LOD was determined at $(2.1 \pm 0.1) \times 10^{-8}$ M. The sensitivity of the modified electrode towards the oxidation of DA was found to be 0.289 μA μM^{-1}. The sensor was applied to determine DA within real specimens.[140]

Beitollahi and Sheikhshoaie reported an adjusted CPE by implementing CNT and a molybdenum(VI) complex. CV was used to characterize the adjusted electrode. This electrode exhibited favorable electrocatalytic impact towards EP oxidation. When applying DPV, the EP peak currents reported in pH 7 linearly depended on concentrations of 0.09–750.0 μM range and 49 nM LOD regarding EP. The sensitivity of EP was found to be 0.3115 μA μM^{-1}. This electrode was applied to determine EP in EP ampoules.[141]

Tavana *et al.* described a hydrophilic ionic liquid 1-methyl-3-butylimidazolium bromide [MBIDZ] Br modified carbon nanotubes paste electrode (CNTPE). The EP electrochemical activity at the reformed electrode was examined at pH 7 phosphate buffer solution (PBS). The EP DPV current was linearly increased across the 0.3–450 μM concentration range. The associated LOD for EP was 0.09 μM. The sensitivity was determined at 0.01670 ± 0.0022 μA μM^{-1} EP. This electrode was used to determine EP and AC within human urine as well as serum and pharmaceutical specimens with satisfactory results.[142]

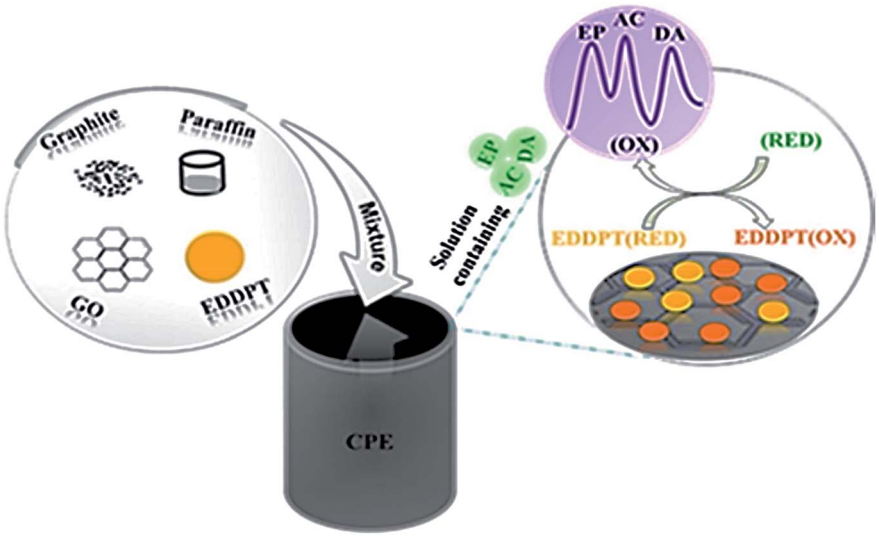

Fig. 2 Schematic representation of the CPE modified with GO and EDDPT as modifiers simultaneous determination of EP, AC and DA. Reprinted with permission from ref. 143 Copyright (2017) Elsevier.

Open Access Article. Published on 04 June 2020. Downloaded on 11/7/2025 11:42:49 AM. This article is licensed under a Creative Commons Attribution-NonCommercial 3.0 Unported Licence.

Dehghan Tezerjani *et al.* proposed an electrochemical sensor to determine EP on the basis of CPE adjusted using GO and 2-(5-ethyl-2,4-dihydroxyphenyl)-5,7-dimethyl-4*H*-pyrido[2,3-d][1,3] thiazine-4-one (EDDPT) as modifiers as depicted in Fig. 2. At optimal conditions, there was a reduction of 279 mV in terms of EP oxidation over potential at the adjusted CPE compared to the non-adjusted CPE. The associated linear range and LOD of EP was determined as 1.5–600.0 μM and 0.65 μM, correspondingly by applying the sensor and DPV approach. The electrochemical sensor showed an excellent sensitivity of 0.22 μA μM^{-1}.[143]

Mazloum Ardakani *et al.* proposed a CPE altered using 2,2′-[1,2 butanediylbis(nitriloethylidyne)]-bishydroquinone (BBNBH) and TiO_2 nanoparticles for EP voltammetric determination. The electrochemical reaction properties of the reformed electrode concerning AC and EP was examined using the DPV and CV approaches. There was an efficient catalytic behavior exhibited by the electrode regarding EP electro-oxidation that entails an overpotential decrease of over 270 mV. At pH 8 optimal state within a 0.1 M PBS, there was a linear relation displayed by the DPV anodic peak compared to EP concentrations across the 1.0–600.0 μM range and 0.2 μM detection limit. The sensitivity of the sensor was estimated to be 0.486 μA μM^{-1}.[144]

Mazloum Ardakani *et al.* fabricated a CPE adjusted with ZrO_2 nanoparticles and applied it to examine EP, AC, folic acid (FA) electro-oxidation including relevant mixtures using electrochemical approach. The resulting differences among EP–AC, AC–FA and EP–FA were 210 mV, 290 mV and 500 mV, correspondingly. The EP DPV peak current exhibited linear enhancement across the 2.0×10^{-7} to 2.2×10^{-3} M concentration range. The EP LOD was determined as 9.5×10^{-8}. The sensitivity (0.016 μA μM^{-1}) of sensor was estimated from the slope of calibration curve.[145]

Pahlavan *et al.* explained nanocomposite (ZnO/CNTs) room temperature ionic liquid (1,3-dipropylimidazolium bromide) adjusted CPE application and synthesis as a voltammetric sensor to ascertain noradrenaline (NE) within biological and pharmaceutical specimens. The SWV method was used as a sensitive electrochemical approach to determine NE. There was a linear response range of 5.0×10^{-8} to 4.5×10^{-4} M with a LOD of 2.0×10^{-8} M. The sensitivity (2.9464 μA μM^{-1}) of sensor was determined. This sensor was used to determine NE in ampoule specimens and athlete urine samples with satisfactory results.[146]

Mazloum Ardakani *et al.* reported ZrO_2 nanoparticles adjusted CPE to examine NE, AC and FA electro-oxidation including associated mixtures using electrochemical approaches. The NE DPV peak currents exhibited linear increases across the 1.0×10^{-7} to 2.0×10^{-3} M concentration range and 8.95×10^{-8} M detection limit. The electrode showed a sensitivity of 0.0153 μA μM^{-1}. The electrode exhibited significant functionality to resolve the overlap voltammetric reactions of NE, FA and AC into three clarified voltammetric peaks.[147]

Mahmoudi Moghaddam and Beitollahi described an adjusted carbon nanotube paste electrode (CNPE) using ferrocene dicarboxylic acid (FCD) which was applied for selective and sensitive voltammetric ascertaining of NE. At optimal state, the NE calibration curve was acquired across the 0.03–500.0 μM range and 22.0 nM LOD (3σ) by implementing DPV. The sensitivity of the modified electrode towards the oxidation of NE was found to be 0.059 μA μM^{-1}. The DPV method was applied to concurrently ascertain AC and NE at the adjusted electrode as well as the quantitation of AC and NE within real specimens using the standard addition method.[148]

Mazloum Ardakani *et al.* examined the NE and UA, D-penicillamine (D-PA) electro-oxidation along with relevant mixtures by adjusted CNPE for 2,2′-[1,2-ethanediylbis (nitriloethylidyne)]-bis-hydroquinone (EBNBH). The linear calibration plot was acquired across the 0.1–1100.0 μM concentration range for NE. The sensitivity of the sensor was estimated to be 0.1555 μA μM^{-1}. The outcomes were described by the electrocatalytic responses theory at chemically adjusted electrodes.[149]

Afkhami *et al.* documented polyglycine microparticles' electrodeposition into zinc oxide nanoparticles/MWCNT-adjusted CPE surface for the purpose of creating levodopa (LD) electrochemical sensor. Under optimal state, the LD concentration was ascertained by the DPV method and LOD of 0.08 μM across 5.0–500.0 μM concentration range was achieved. The sensitivity (0.173 μA μM^{-1}) was estimated for oxidation peak.[150]

Beitollahi *et al.* conducted a study to modify a CPE using 2,7-bis(ferrocenyl ethyl)fluoren-9-one (2,7-BF) and CNT for sensitive voltammetric ascertaining LD. The electrochemical reaction properties for the adjusted electrode in regard to LD, UA and FA was examined. The outcomes exhibited efficient catalytic behavior concerning the electrode for LD electro-oxidation that entails a reduction of 320 mV in terms of overpotential. The linear range (0.1–700.0 μM), LOD (58 nM) and sensitivity (0.4353 μA μM^{-1}) were estimated for oxidation peak. This electrode was applied to ascertain LD within real specimens.[151]

Tajik *et al.* examined LD electrochemical oxidation at CPE adjusted surface using graphene nanosheets, 1-(4-bromobenzyl)-4-ferrocenyl-1*H*-[1,2,3]-triazole (1,4-BBFT) and hydrophilic ionic liquid (*n*-hexyl-3-methylimidazolium hexafluoro phosphate) as a binder. They concluded that LD oxidation at the adjusted modified electrode surface took place at approximately 210 mV potential less positive compared to an unadjusted CPE. The measured current using the SWV method proved favorable linear characteristic as LD concentration function across the 5.0×10^{-8} to 8.0×10^{-4} M range. The LOD of LD was found to be 1.5×10^{-8} M and 0.58 μA μM^{-1} sensitivity.[152]

Santos *et al.* concurrently determined LD, PRX, ofloxacin (OFX) and methocarbamol (MCB) at CPE adjusted using graphite oxide (GrO) and β-cyclodextrin (CD). At optimal state, the associated SWV currents for LD, PRX, OFX and MCB exhibited a linear increase with relevant concentrations across the 1.0 to 20 μM, 1.0 to 15 μM, 1.0 to 20 μM and 1.0 to 50 μM ranges, correspondingly. The detection limits of LD, PRX, OFX and MCB were 0.065, 0.105, 0.089 and 0.398 μM, correspondingly. Also, sensitivities of 3.05, 3.06, 5.37 and 0.42 μA μM^{-1} cm^{-2} achieved for LD, PRX, OFX and MCB respectively.[153]

Beitollahi *et al.* studied electrocatalytic oxidation of LD by reformed CNPE of graphene and ethyl 2-(4-ferrocenyl-[1,2,3] triazol-1-yl) acetate (EFTA). The acquired catalytic peak current exhibited linear dependency on LD concentrations across the 0.2 μM to 0.4 mM range and 0.07 μM LD detection limit,

Open Access Article. Published on 04 June 2020. Downloaded on 11/7/2025 11:42:49 AM.
This article is licensed under a Creative Commons Attribution-NonCommercial 3.0 Unported Licence.

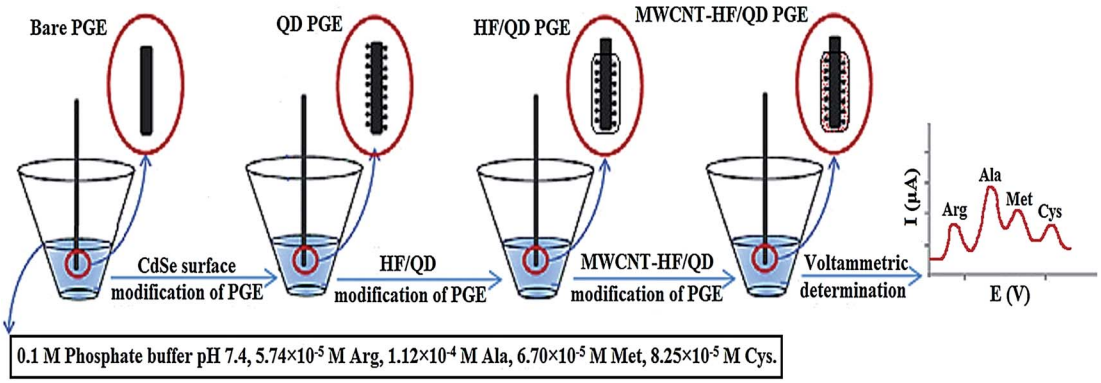

Fig. 3 Schematic of preparation of different modified electrodes with CdSe QD modified/MWCNT in 4 steps. Reprinted with permission from ref. 160 Copyright (2017) Elsevier.

correspondingly. The electrode showed a sensitivity of 1.082 μA μM^{-1} cm^{-2}. The modified electrode can well resolve the voltammetric peaks of LD, AC and Tyr.[154]

Amino acids. Amino acids are known for being biologically vital substances which are extensively spread in numerous plants and animals as protein components. Amino acids are associated to the functionalities of biological active proteins, namely hormones and enzymes.[155–157]

Yang *et al.* reported an electrochemical sensor on the basis of using Y_2O_3 nanoparticles supported on nitrogen-doped reduced graphene oxide (N-rGO) for L-cysteine. There was a linear increase for the current which was determined at 0.7 V potential *vs.* Ag/AgCl within the 1.3 to 720 μM concentration range for L-cysteine at 0.8 μM detection limit. The sensitivity of the sensor was estimated to be 12.33 μA μM^{-1}. This sensor was used to determine L-cysteine within spiked syrup with satisfactory results.[158]

Kumar Gupta *et al.* examined MgO nanoparticle electrical conductivity impact and acetylferrocene (AF) electro-catalytic impact to modify CPE as a significantly sensitive electrochemical sensor to electro-catalytically ascertain L-cysteine within an aqueous solution. The adjusted electrode exhibited favorable electro-catalytic behavior to analyze L-cysteine across a 0.1–700.0 μM concentration range and 30.0 nM LOD by applying the DPV approach. The adjusted electrode showed a sensitivity of 0.0388 μA μM^{-1}.[159]

Hoshmand and Eshaghi concurrently determined four amino acids at CPE adjusted using CdSe QD in addition to a MWCNT within various bodybuilding supplements as shown in Fig. 3. Arginine, methionine, alanine and cysteine electro-oxidation at the adjusted electrode surface were examined. At optimal state, the associated DPV currents for alanine, arginine, methionine and cysteine exhibited a linear increase with relevant concentrations across the 0.287 to 33 670 μM range. The detection limits were 0.158, 0.081, 0.094 and 0.116 μM, correspondingly. The sensitivity (11.47 μA μM^{-1}, 17.62 μA μM^{-1}, 8.23 μA μM^{-1} and 6.69 μA μM^{-1}) of sensor for arginine, alanine, methionine and cysteine were calculated.[160]

Karami and Sheikhshoaie proposed a prompt electrochemical Tyr sensor on the basis of CPE adjusted using reduced graphene oxide (rGO)/zinc oxide nanocomposite. The Tyr anode peak current exhibited an increase at 0.1–400 μM concentration range for this amino acid. The LOD was 0.07 μM. The sensitivity was determined at 0.0829 μA μM^{-1}. The electrode performance was assessed to analyze Tyr within pharmaceutical serum specimens and water.[161]

Wei *et al.* reported an adjusted CPE for Tyr sensitive detection within human serum which was constructed using glycine polymer and MWCNTs as depicted in Fig. 4. *In situ* electrochemical polymeric disposition was used to prepare glycine polymer. At optimal state, the linear sweep voltammetry value for the oxidation peak exhibited linear relation across the 0.2–400 μM range and 0.07 μM (S/N = 3) detection limit. The adjusted CPE showed a sensitivity of 1.031 μA μM^{-1}.[162]

Karimi and Heydari suggested a sensor on the basis of CPE reformed using mesoporous silica nanoparticles (MSNPs) to ascertain Tyr and Trp. Upon optimizing experimental factors, TRP oxidation peak current exhibited linear activity across the 0.05 to 600 μM concentration range and 1.13×10^{-8} M detection peak. Likewise, Tyr concentration range on the basis of the oxidation peak current was within the 0.3–600 μM range with

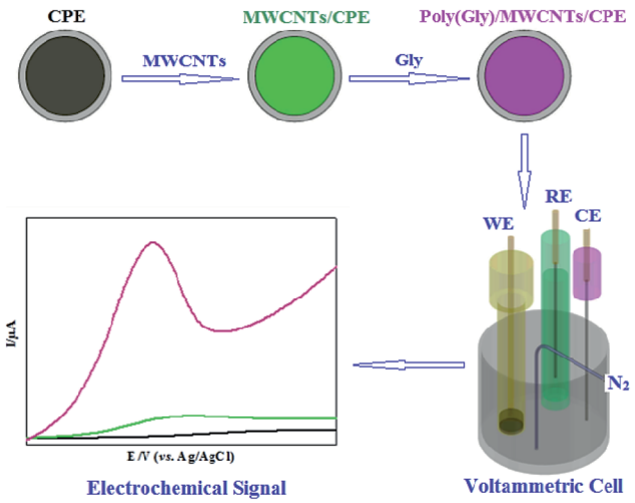

Fig. 4 Schematic illustration of glycine polymer and MWCNTs/CPE fabrication. Reprinted with permission from ref. 162 Copyright (2018) Electrochemical Science Group, University of Belgrade.

Open Access Article. Published on 04 June 2020. Downloaded on 11/7/2025 11:42:49 AM. This article is licensed under a Creative Commons Attribution-NonCommercial 3.0 Unported Licence.

4.97×10^{-8} M detection limit. The results showed the high sensitivities of 599.3 μA μM^{-1} and 113.4 μA μM^{-1} for Trp and Tyr, respectively. The suggested method is potentially competent to simultaneously determine these amino acids. This was confirmed by artificial urine analysis as a real sample.[163]

Ghoreishi and Malekian conducted a DPV study which proved significant voltammograms' overlapping for Tyr and Trp oxidation. An electrochemical sensor was fabricated using $ZnFe_2O_4$ nanoparticles adjusted CPE. The suggested approach was used at an optimal state to ascertain Tyr and TRP within the 0.1–200.0 μM and 0.4–175.0 μM linear ranges and 0.10 μM and 0.04 μM detection limits, correspondingly (S/N = 3). Moreover, adjusted CPE exhibited much high sensitivity of 76.0 and 95.4 μA mM^{-1} for Tyr and Trp, respectively. This approach was implemented to simultaneously determine Tyr and TRP within urine samples and spiked human serum.[164]

Zeinali *et al.* reported the fabrication of a sensor to concurrently ascertain melatonin (MT) and TRP. This sensor consisted of an ionic liquid CPE adjusted with reduced graphene oxides decorated with SnO_2–Co_3O_4 nanoparticles. At optimal testing state, the linear response was acquired within the 0.02 to 6.00 μM concentration range and 3.2 and 4.1 nM LOD for TRP and MT, correspondingly. Moreover, sensor exhibited sensitivity of 9.254 and 12.858 μA μM^{-1} for MT and TRP, respectively. The functionality of the suggested sensor was approved by assessing TRP and MT within different real specimens such as tablet samples and human serum.[165]

Mazloum Ardakani *et al.* reported a CPE which was chemically adjusted using TiO_2 nanoparticles and quinizarine (QZ) adopting the role of an electrochemical sensor to concurrently determine scarce quantities of D-PA and Trp. The D-PA oxidation peak potential was decreased by a minimum of 220 mV in comparison to that of unadjusted CPEs. Under optimal state, the linear range for D-PA was 0.8 to 140.0 μM and the LOD was 0.76 μM. The sensor displayed 0.0647 μA μM^{-1} sensitivity.[166]

Others. Ensafi and Karimi-Maleh fabricated an electrochemical approach to determine isoproterenol (IP) by utilizing MWCNT as well as room temperature ionic liquid. At optimal state, there was a linear peak current to IP concentration within the 1.0 to 520 μM concentration range *via* the DPV approach. A LOD of 0.85 μM was determined. The sensitivity was determined at 0.1016 μA μM^{-1}. The suggested method was used to determine IP within urine and ampoules with satisfactory results.[167]

Beitollahi *et al.* conducted a study where a CPE adjusted using CNTs and 5-amino-3′,4′-dimethylbiphenyl-2-ol (5ADB) was applied to develop an electrochemical sensor to determine IP at the vicinity of *N*-acetylcysteine (NAC) and AC. At optimal state, pH 7, IP oxidation took place at 215 mV potential less positive compared to that of unadjusted CPEs. The catalytic current reaction with IP concentration exhibited a linear relationship within the 4.0×10^{-7} to 9.0×10^{-4} M concentration range and 2.0×10^{-7} M detection limit. The sensitivity of the modified electrode toward the oxidation of IP was found to be 0.0311 μA μM^{-1}. This is very close to the value obtained in the absence of AC and NAC (0.0325 μA μM^{-1}).[168]

Tajik *et al.* synthesized a ferrocene derivative compound, 1,4-BBFT which was implemented to develop an adjusted graphene paste electrode. The binder applied to develop the adjusted electrode was hydrophilic ionic liquid (*n*-hexyl-3-methylimidazolium hexafluoro phosphate). SWV and CV methods were used to examine IP electro-oxidation at the adjusted electrode surface. At optimal state, the IP SWV peak current displayed a linear increase with IP concentration within the 6.0×10^{-8} to 7.0×10^{-4} M concentration range and 12.0 nM LOD for IP. The sensitivity of the modified electrode toward the oxidation of IP was found to be 0.731 μA M^{-1}. The fabricated electrode displayed favorable resolution among the IP, AC and theophylline voltammetric peaks making it beneficial to detect IP at the vicinity or theophylline and AC within real specimens.[169]

Ensfi and Karimi-Maleh proposed a ferrocenemonocarboxylic acid (FMA) modified CNTPE and applied it for prompt and sensitive IP determination at trace levels. By implementing the DPV method, a broad linear range of 0.5–50.0 μM at 0.2 μM LOD was acquired for IP. The sensitivity was determined at 2.1045 μA μM^{-1}.[170]

Beitollahi *et al.* described IP selective determination with the existence of UA and FA by utilizing 2,7-BF adjusted CNPE (2,7-BFCNPE) within 0.1 M phosphate buffer solution, pH 7.0. Concerning PBS at pH 7, there was linear increase of oxidation current with IP concentration intervals from 0.08 to 700.0 μM. DPV was applied to determine the LOD (3σ) of 26.0 ± 2 nM. The plot of peak current *vs.* IP concentration showed a sensitivity of 0.5206 μA μM^{-1}. Pragmatic uses of the electrode were displayed by ascertaining IP within urine, IP injections and human blood serums.[171]

Karimi Maleh *et al.* reported a MWCNT adjusted electrode using *p*-chloranil which adopted the role of a mediator as a voltammetric sensor to determine methyldopa (MD) with the existence of UA. The findings show efficient electrode performance regarding its electrocatalytic behavior for MD oxidation causing a decrease in overpotential of over 250 mV. Within the 0.5–165.5 μM concentration range, the peak current exhibited linear dependency on MD. The LOD was 0.2 μM (with a sensitivity of 0.1133 μA μM^{-1}) in the SWV. This electrode was applied to determine MD in serum, drug and urine specimens by implementing the standard addition method.[172]

Tajik *et al.* explained an electrochemical mechanism for MD voltammetric oxidation at CPE adjusted using 5-amino-2′-ethylbiphenyl-2-ol (5AEB) and CNTs. The findings showed that at the adjusted electrode surface, the MD voltammetric reaction was distinctly improved whilst the MD oxidation took place at an overpotential of 220 mV less positive compared to that of an unadjusted CPE at the surface of the adjusted electrode. The SWV method was used to measure the current which exhibited favorable linear characteristic as a function of MD concentration within the 0.1–210.0 μM range and 48.0 nM LOD for MD. The sensitivity of the modified electrode towards the oxidation of MD was found to be 0.4348 μA μM^{-1}.[173]

Alizadeh *et al.* described an electrochemical sensor for the opioid drug buprenorphine. Molecularly imprinted polymer (MIP) nanoparticles were prepared. The resulting polymer along

Open Access Article. Published on 04 June 2020. Downloaded on 11/7/2025 11:42:49 AM.
This article is licensed under a Creative Commons Attribution-NonCommercial 3.0 Unported Licence.

Table 1 Selected applications of CPEs in biological species and pharmaceuticals compounds analysis using DPV

Analyte	Modifier	Linear range	Detection limit	Ref.
Glutathione	Trichloro(terpyridine)ruthenium(III)/multi-wall carbon nanotubes (TChPRu-MWCNT)	0.6–56.8 μM	0.3 μM	122
Gallic acid	SiO_2 nanoparticles	8.0×10^{-7} to 1.0×10^{-4} M	2.5×10^{-7} M	127
Gallic acid	Zirconia nanoparticles/choline chloride/gold nanoparticles (ZrO_2NPs–ChCl–AuNPs)	0.22–55 μM	25 nM	128
Gallic acid	TiO_2 NPs	2.5×10^{-6} to 1.5×10^{-4} M	9.4×10^{-7} M	129
Citric acid	MIL-101(Fe)	5.0 to 100 μM	4.0 μM	130
Dopamine	*N*,*N*′(2,3-Dihydroxybenzylidene)-1,4-phenylenediamine (DHBPD) and TiO_2 nanoparticles	0.08–20.0 μM	3.14×10^{-8} M	138
Dopamine	Graphene oxide (GO)/lanthanum (La) complex	0.01–400.0 μM	0.32 nM	139
Epinephrine	Carbon nanotube (CNT)/molybdenum(VI) complex (MC)	0.09 to 750.0 μM	49 nM	141
Epinephrine	Hydrophilic ionic liquid 1-methyl-3-butylimidazolium bromide [MBIDZ]Br/carbon nanotube (CNT)	0.3–450 μM	0.09 μM	142
Epinephrine	Graphene oxide (GO)/2-(5-ethyl-2,4-dihydroxyphenyl)-5,7-dimethyl-4*H*-pyrido[2,3-*d*][1,3]thiazine-4-one (EDDPT)	1.5–600.0 μM	0.65 μM	143
Epinephrine	2,2′-[1,2-Butanediylbis(nitriloethylidyne)]-bishydroquinone (BBNBH)/TiO_2 nanoparticles	1.0–600.0 μM	0.2 μM	144
Epinephrine	ZrO_2 nanoparticles	2.0×10^{-7} to 2.2×10^{-3} M	9.5×10^{-8} M	145
Norepinephrine	ZrO_2 nanoparticles	1.0×10^{-7} to 2.0×10^{-3} M	8.95×10^{-8} M	147
Norepinephrine	Ferrocene dicarboxylic acid (FCD)/carbon nanotube(CNT)	0.03–500.0 μM	22.0 nM	148
Norepinephrine	2,2′-[1,2-Ethanediylbis (nitriloethylidyne)]-bis-hydroquinone (EBNBH)/carbon nanotube(CNT)	0.1–1100.0 μM	8.2×10^{-8} M	149
Levodopa	Polyglycine/zinc oxide nanoparticles/multi-walled carbon nanotubes PG/ZnO/MWCNTs	5.0–500.0 μM	0.08 μM	150
Levodopa	2,7-Bis(ferrocenylethyl)fluoren-9-one (2,7-BF)/carbon nanotube (CNT)	0.1–700.0 μM	58 nM	151
L-Cysteine	MgO nanoparticle/acetylferrocene (AF)	0.1–700.0 μM	30.0 nM	159
Arginine	CdSe quantum dot (QD)/multi-walled carbon nanotube (MWCNT)	0.287 to 33 670 μM	0.081 μM	160
Alanine			0.158 μM	
Methionine			0.094 μM	
Cysteine			0.116 μM	
Tryptophan	Mesoporous silica nanoparticles (MSNs)	0.05–600 μM	1.13×10^{-8} M	163
Tyrosine		0.3–600.0 μM	4.97×10^{-8} M	
Tryptophan	$ZnFe_2O_4$ nanoparticles	0.1–200.0 μM	0.04 μM	164
Tyrosine		0.4–175.0 μM	0.10 μM	
Melatonin	SnO_2–Co_3O_4@rGO nanocomposite/ionic liuid (SnO_2–Co_3O_4@rGO/IL)	0.02–6.00 μM	4.1 nM	165
Tryptophan		4.1–3.2 nM	3.2 nM	
Isoproterenol	Multiwall carbon nanotube (MWCNT)/ionic liquid (1-butyl-3-methylimidazolium hexafluoro phosphate ([C_4mim]-[PF_6])) (IL)	1.0–520 μM	0.85 μM	167
Isoproterenol	1-(4-Bromobenzyl)-4-ferrocenyl-1*H*-[1,2,3]-triazole (1,4-BBFT)/hydrophilic ionic liquid (*n*-hexyl-3-methylimidazolium hexafluoro phosphate)/graphene (1,4-BBFT/IL/G)	6.0×10^{-8} to 7.0×10^{-4} M	12.0 nM	169
Isoproterenol	Ferrocenemonocarboxylic acid (FMA)/carbon nanotube (CNT)	0.5–50.0 μM	0.2 μM	170
Isoproterenol	2,7-Bis(ferrocenyl ethyl)fluoren-9-one (2,7-BF)/carbon nanotube (CNT)	0.08–700.5 μM	26.0 ± 2 nM	171
Buprenorphine	Molecularly imprinted polymer (MIP)/nanoparticles multiwalled carbon nanotubes (MWCNTs)	1 nM to 50 μM	0.6 nM	174
Acetaminophen	Zinc ferrite nanoparticles ($ZnFe_2O_4$ NPs)	6.5–135 μM	0.4 μM	175
Epinephrine		5–100 μM	0.7 μM	
Melatonin		6.5–145 μM	3.0 μM	
Melatonin	Al_2O_3-supported palladium nanoparticles	6.0 nM to 1.4 mM	21.6 nM	176
Dopamine		50 nM to 1.45 mM	36.5 nM	
Acetaminophen		40 nM to 1.4 mM	36.5 nM	

with MWCNT was used to fabricate the modified CPE which exhibited an anodic peak at about +0.73 V (*vs.* Ag/AgCl) for buprenorphine. The MIP on the CPE exhibited a favorable detection 0.6 nM across a 1 nM to 50 μM linear dynamic range. The sensitivity was determined at 2.0918 μA mM^{-1}.[174]

Tavakkoli *et al.* fabricated an electrochemical approach to concurrent determine AC, EP, and MT by utilizing a modified

Open Access Article. Published on 04 June 2020. Downloaded on 11/7/2025 11:42:49 AM. This article is licensed under a Creative Commons Attribution-NonCommercial 3.0 Unported Licence.

Table 2 Selected applications of CPEs in biological species and pharmaceuticals compounds analysis using SWV

Analyte	Modifier	Linear range	Detection limit	Ref.
Glutathione	*N*-(4-Hydroxyphenyl)-3,5-dinitrobenzamide-FePt/carbon nanotube (NHPDA/FePt/CNTs)	0.004–340 μM	1.0 nM	121
Glutathione	MgO/SWCNTs/2-chloro-*N*′-[1-(2,5-dihydroxyphenyl) methylidene]aniline (2-CDHPMA)	0.05–700.0 μM	10 nM	123
Glutathione	Ag–ZnO nanoplates/2-chlorobenzoyl ferrocene (2-CBF)	5.0×10^{-8} to 2.0×10^{-4} M	20.0 nM	124
Glutathione	Ethynylferrocene (EF)/NiO/MWCNT nanocomposite	0.01–200 μM	0.006 μM	125
Dopamine	CdTe quantum dots	7.5×10^{-8} to 6.0×10^{-4} M	2.1×10^{-8} M	140
Norepinephrine	ZnO/CNTs nanocomposite/ionic liquid (1,3-dipropylimidazolium bromide) (ZnO/CNTs/IL)	5.0×10^{-8} to 4.5×10^{-4} M	2.0×10^{-8} M	146
Levodopa	Graphene nanosheets, 1-(4-bromobenzyl)-4-ferrocenyl-1*H*-[1,2,3]-triazole (1,4-BBFT) and hydrophilic ionic liquid (*n*-hexyl-3-methylimidazolium hexafluoro phosphate)	5.0×10^{-8} to 8.0×10^{-4} M	1.5×10^{-8} M	152
Levodopa	Graphite oxide (GrO) and β-cyclodextrin (CD)	1.0–20 μM	0.065 μM	153
Levodopa	Graphene/ethyl 2-(4-ferrocenyl-[1,2,3]triazol-1-yl) acetate (EFTA)	0.2–0.4 mM	0.07 μM	154
Tyrosine	Reduced graphene oxide (rGO)/zinc oxide nanocomposite	0.1–400 μM	0.07 μM	161
D-Penicillamine	TiO_2 nanoparticles/quinizarine (QZ)	0.8–140.0 μM	0.76 μM	166
Isoproterenol	5-Amino-3′,4′-dimethyl-biphenyl-2-ol (5ADB)/carbon nanotube	4.0×10^{-7} to 9.0×10^{-4} M	2.0×10^{-7} M	168
Methyldopa	Multiwalled carbon nanotubes (MWCNT)/*p*-chloranil	0.5–165.5 μM	0.2 μM	172
Methyldopa	5-Amino-2′-ethyl-biphenyl-2-ol (5AEB)/carbon nanotubes (CNTs)	0.1–210.0 μM	48.0 nM	173

CPE with zinc ferrite nanoparticles ($ZnFe_2O_4$ NPs). Within the concentration range of 6.5–135 μM for AC, 5–100 μM for EP, and 6.5–145 μM for MT, linear calibration curves were achieved. The detection limits are 0.4 μM for AC, 0.7 μM for EP, and 3.0 μM for MT. The sensitivities are 0.0313 μA μM^{-1} for AC, 0.0281 μA μM^{-1} for EP, and 0.0204 μA μM^{-1} for MT.[175]

Soltani *et al.* reported the fabrication of a sensor to concurrently ascertain MT, DA and AC. This sensor consisted of a CPE with Al_2O_3-supported palladium nanoparticles. The suggested approach was used at an optimal state to ascertain DA, AC and MT within the 50 nM to 1.45 mM, 40 nM to 1.4 mM, and 6.0 nM to 1.4 mM linear ranges and 36.5 nM, 36.5 nM and 21.6 nM detection limits, correspondingly (S/N = 3). The sensitivities are 1.001 μA μM^{-1} cm^{-2} for MT, 0.0429 μA μM^{-1} cm^{-2} for DA, and 0.490 μA μM^{-1} cm^{-2} for AC. This approach was implemented to determine analytes in (spiked) human serum and drug samples.[176]

The application of CPEs within pharmaceuticals compound and biological species analysis by DPV, SWV and chronoamperometry (CHA), amperometry, linear sweep voltammetry (LSV) are surveyed in Tables 1, 2 and 3, respectively. Summarized data present the progression and individual trends mentioned previously.

Environment pollution

Pesticides. Pesticides (insecticides, fungicides, herbicides) are extensively applied worldwide and millions of tons are applied annually in the industry, namely the agricultural and medicine fields. Identical compounds create possible nerve poisons, thus they are also used in the military. Several of them are extremely toxic, and when aggregated, may cause severe diseases in living organisms.[177–181]

Demir and Inam proposed CV and SWV methods to derive the electrochemical activities of fomesafen herbicide on modified CNPE. Electrochemical assessments indicated that the $-NO_2$ group caused the reduction procedure. Within the 0.30–40 mg L^{-1} concentration range, a linear correlation was evident. The detection limits and quantification values were found to be 0.089 and 0.297 mg L^{-1}, correspondingly. The sensitivity (0.370 μA mg^{-1} L^{-1}) of sensor was estimated from the slope of calibration curve. With the existence of a few renowned pesticides, fomesafen was ascertained with 5 mg L^{-1} fomesafen recoveries with the existence of anilazine, pymetrozine and triflumizole pesticides in equal amounts to be 103.7 ± 0.9, 94.3 ± 0.4, and 97.9 ± 0.5%, correspondingly ($n = 3$).[182]

Parham *et al.* reported a CPE altered using ZrO_2-nanoparticles for SWV detection of methyl parathion (MP). There was a linear increase in terms of SWV peak current at 5.0–3000.0 ng mL^{-1} concentration range and 2.0 ng mL^{-1} detection limit, correspondingly. The sensitivity of the proposed method was 1.3641 μA μg^{-1} mL^{-1} for MP. The altered electrode was applied with favorable results to determine MP in different water samples.[183]

Zahirifar *et al.* produced an electrochemical sensor on the basis of CNTs adjusted CPE to determine diazinon (DZN). The relevant electrocatalytic currents displayed linear enhancement

Open Access Article. Published on 04 June 2020. Downloaded on 11/7/2025 11:42:49 AM. This article is licensed under a Creative Commons Attribution-NonCommercial 3.0 Unported Licence.

Table 3 Selected applications of CPEs in biological species and pharmaceuticals compounds analysis using CHA, amperometry and LSV

Analyte	Modifier	Electrochemical method	Linear range	Detection limit	Ref.
Ascorbic acid	4-Aminobenzoic acid/herringbone carbon nanotubes (4ABA–hCNTs)	CHA	0.065–1000.0 μM	0.065 μM	126
Selegiline Pramipexole	Nickel nanoparticles	Amperometry	5×10^{-6} to 1×10^{-4} 5×10^{-8} to 1×10^{-6}	4.0×10^{-6} M 4.5×10^{-8} M	137
L-Cysteine	Y_2O_3 nanoparticles supported on nitrogen-doped reduced graphene oxide (N-rGO)	Amperometry	1.3 to 720 μM	0.8 μM	158
Tyrosine	Glycine polymer/multi-walled carbon nanotubes (MWCNTs)	LSV	0.2–400 μM	0.07 μM	162

within 1×10^{-10} to 6×10^{-8} M DZN concentration range and 4.5×10^{-10} M LOD for DZN. The sensitivity of the electrochemical sensor was 18.973 μA μM^{-1} for DZN. The developed electrode was applied to determine DZN within food samples.[184]

Heavy metals. Heavy metal contamination is detrimental to human health, ecological systems and living resources. Theses metals are not biodegradable and are inclined to pile up within living organisms, which cause several disorders and diseases in the gastrointestinal, reproductive, immune and nervous systems.[185–187] Heavy metal pollution is a prominent environmental issue due to their stability in polluted sites and the complicated process of biological toxicity. When these metals are absorbed, they are aggregated inside the body and are damaging to human health.[188–191] Thus, focus is on developing a greatly sensitive approach to determine trace quantities of heavy metal ions.

Niu *et al.* described a comprehensive analytical evaluation of bismuth nanoparticle porous CPE used as an electrochemical sensor to detect Cd(II), Pb(II) and Ni(II) within water specimens of various origins. The detection limits for Cd(II), Pb(II) and Ni(II) were 0.81, 0.65 and 5.47 ppb, correspondingly. The total analysis period was under 240 seconds. The sensitivity of the sensor was estimated to be 0.19 ± 0.04, 0.13 ± 0.02 and 0.04 ± 0.01 μA ppb^{-1} for Cd(II), Pb(II) and Ni(II), respectively. The sensor was used to analyze numerous inconsistent specimens, namely ground water, tap water, and contaminated water from effluent and influent urban wastewater treatment station including contaminated river water because of acid mine drainage.[192]

Chemical synthesis was conducted on a nanocomposite on the basis of MWCNT adjusted using antimony nanoparticles (SbNPs) which was implemented to produce an electrode by utilizing carbon paste as a substrate. This electrode was used to determine Pb^{2+} and Cd^{2+} using the square wave adsorptive stripping voltammetry (SWASV) method. The associated detection limits for the analytes were 0.77 μg L^{-1} and 0.65 μg L^{-1} for Cd^{2+} and Pb^{2+}, correspondingly. Sensitivities of 0.2411 μA μg^{-1} L^{-1} for Pb^{2+} and 0.1628 μA μg^{-1} L^{-1} for Cd^{2+} were also evaluated.[193]

Devnani and Satsangee synthesized AuNPs and assessed their uses in developing Au NP adjusted CPE based on anthocyanin to ascertain heavy metal quantities. This metal sensor was applied to determine cadmium, copper and lead by applying the square wave anodic stripping voltammetry method. CV and electrochemical impedance spectroscopy were implemented to specify the sensor. Within the concentration range of 50–500 μg L^{-1} for lead and 200–700 μg L^{-1} for cadmium and copper, linear calibration curves were achieved. This sensor exhibited minimum detection limits to electrochemically ascertain lead, cadmium and copper *i.e.* 9.178, 86.327 μg L^{-1} and 85.373 μg L^{-1}, correspondingly. Sensitivities of 0.5014 μA μg^{-1} L^{-1} for Pb^{2+}, 0.0923 μA μg^{-1} L^{-1} for Cd^{2+} and 0.0778 μA μg^{-1} L^{-1} for Cu^{2+} were also evaluated.[194]

Roushani *et al.* reviewed the development and specifications of a sensitive electrochemical sensor to efficiently detect cadmium ion *via* a metal–organic structure. The modifier used for this approach was graphene/TMU-16-NH_2([$Zn_2(NH_2$-BDC$)_2$(4-bpdh)]·3DMF) metal–organic framework (graphene/MOF(TMU-16-NH_2)). The intercommunications between the TMU-16-NH_2 cadmium and amine groups are modified *via* dative attachment causing Cd^{2+}–N complexation originating from soft–soft interactions. At optimal testing state, when adding cadmium to the sample, the oxidation current was increased and DPV was used to achieve dynamic range from 0.7 to 120 μg L^{-1}. A low LOD of 0.2 μg L^{-1} was displayed. The electrochemical sensor exhibited a sensitivity of 0.0967 μA μg^{-1} L^{-1}.[195]

Afkhami *et al.* fabricated a chemically adjusted electrode to simultaneously determine Cu(II) and Cd(II) *via* the square wave anodic stripping voltammetry method. This electrode was adjusted by adding SiO_2 nanoparticles, covered with a newly synthesized Schiff base within the CPE. The detection limits were 0.28 ng mL^{-1} and 0.54 ng mL^{-1} for Cu(II) and Cd(II), correspondingly. The sensitivity was found to be 25.960 μA ng^{-1} mL^{-1} and 10.378 μA ng^{-1} mL^{-1} for Cu(II) and Cd(II), respectively. The suggested chemically adjusted electrode was applied to determine cadmium and copper in numerous foods and water specimens.[196]

Bahrami *et al.* introduced a voltammetric sensor to determine mercury ions *via* carbon ionic liquid paste electrode incorporated with Hg^{2+}-ion imprinted polymetric (IIP) nanobeads on the basis of dithizone, as an adequate ligand for comprehensive creation using Hg^{2+} ions. The performance of the electrode was assessed using the differential pulse anodic stripping voltammetric method to determine dangerous mercury ions. This electrode exhibited linear reactions within the 0.5 nM to 2.0 μM range with 0.1 nM (S/N = 3) detection limit. The sensitivity was found to be 0.032 μA nM^{-1} for Hg^{2+}. The adjusted electrode's peak currents concerning Hg^{2+} ions were highest in phosphate buffer pH 4.5. The determined optimal precondition potential and accumulation period were

Open Access Article. Published on 04 June 2020. Downloaded on 11/7/2025 11:42:49 AM.
This article is licensed under a Creative Commons Attribution-NonCommercial 3.0 Unported Licence.

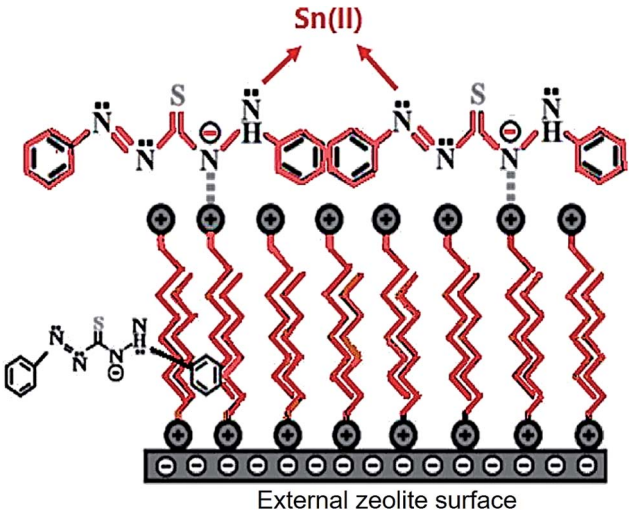

Fig. 5 Schematic representation of the CPE modified with clinoptilolite nano-particles were modified by hexadecyltrimethyl ammonium bromide surfactant and dithizone. Reprinted with permission from ref. 198 Copyright (2017) Elsevier.

−0.9 V and 35 seconds, correspondingly. The sensor was also used to determine mercury in waste water specimens.[197]

Hexadecyltrimethyl ammonium bromide (HDTMA) Br surfactant and dithizone (DZ) were used to modify clinoptilolite nanoparticles, CNP. The resulting zeolite was applied to modify CPE proposed by Niknezhadi and Nezamzadeh-Ejhieh, as shown in Fig. 5. The electrode was then applied to voltammetrically determine Sn(II) within an aqueous solution. Within the 1×10^{-8} to 1×10^{-2} M Sn(II) concentration range with LOD of approximately 9×10^{-9} M Sn(II), the electrode exhibited linear reaction. The sensitivity (14.35 μA μM^{-1}) of sensor was estimated from the slope of calibration curve. The electrode exhibited favorable applicability and selectivity to determine Sn(II) within real specimens, namely a steel firm wastewater, river water, canned tuna fish and tomato paste.[198]

Ghalebi *et al.* synthesized poly(methylene disulfide) nanoparticles (PMDSNPs) and assessed their uses in developing poly(methylene disulfide) nanoparticles (PMDSNPs) adjusted CPE. This adjusted electrode was applied to determine silver(I) by applying the differential pulse anodic stripping voltammetry method. The associated LOD for the silver(I) was 1.0×10^{-13} M. Within the concentration range of 3.0×10^{-12} to 1.0×10^{-9} M for silver(I), linear calibration curves were achieved. The sensitivity was found to be 213.79 μA nM^{-1} for silver(I).[199]

Ghanei-Motlagh *et al.* fabricated a magnetic silver ion imprinted polymer nanoparticle (Fe_3O_4@SiO_2@IIP) on a CPE to electrochemically ascertain silver(I). There was a linear increase in terms of current reaction with silver(I) concentration across the 0.05 to 150 μg L^{-1} concentration range. The associated LOD was 15 ng L^{-1}. The sensitivity was found to be 2.4973 μA ppb^{-1} for silver(I).[200]

Others. Measuring the quantities of compounds such as phenol, sulfite, hydrazine, hydroxylamine, nitrite, and paracetamol is vital in industries.[201–204] Beitollahi *et al.* conducted a study where benzoyl ferrocene (BF) was utilized to create an adjusted graphene paste electrode. The binder used to develop this electrode was hydrophilic ionic liquid (*n*-hexyl-3-methylimidazolium hexafluoro phosphate). Within the 5.0×10^{-8} to 2.5×10^{-4} M concentration range, using SWV, linear dynamic range was exhibited with a 20.0 nM LOD for sulfite. The sensitivity of the modified electrode towards the oxidation of sulfite was found to be 0.077 μA μM^{-1}. The electrode displayed favorable resolution between sulfite and phenol voltammetric peaks, making it suitable to detect sulfite with the existence of phenol within real specimens.[205]

Beitollahi *et al.* reformed a CPE using 2-(4-oxo-3-phenyl-3,4-dihydroquinazolinyl)-*N*′-phenyl-hydrazinecarbothioamide, magnetic core shell Fe_3O_4@SiO_2/MWCNT nanocomposite as well as ionic liquid (*n*-hexyl-3-methylimidazolium hexafluoro phosphate). The hydrazine electro-oxidation at the reformed electrode's surface was examined *via* electrochemical methods. Within the 7.0×10^{-8} to 5.0×10^{-4}M concentration range, SWV displays linear dynamic range and the hydrazine LOD was 40 nM. The sensitivity of the electrode towards the hydrazine was found to be 0.0601 μA μM^{-1}. The electrode displayed favorable resolution among hydrazine and phenol voltammetric peaks, making it beneficial to detect hydrazine with the existence of phenol within real specimens.[206]

Karimi Maleh *et al.* presented a CPE adjusted using ferrocene and carbon nanotubes used as voltammetric sensor to determine sulfite at pH 7. The findings proved that at optimal state, *i.e.* pH 7, using CV, sulfite oxidation takes place at 280 mV potential less positive compared to that of unadjusted CPEs. At optimal state, sulfite electrocatalytic oxidation peak current exhibited linear dynamic range within 0.4–120.0 μM and 0.1 μM LOD for sulfite. The electrode showed a sensitivity of 3.348 μA μM^{-1} for sulfite.[207]

Foroughi *et al.* studied hydroxylamine electrochemical activities at BF adjusted carbon nanotubes paste electrode. The relevant electrocatalytic currents displayed linear enhancement within 0.9–400.0 μM hydroxylamine concentration range and 0.1 μM LOD for hydroxylamine. The sensitivity for hydroxylamine was 0.715 μA μM^{-1}. The electrode was applied to determine hydroxylamine within water specimens.[208]

Mohammadi *et al.* conducted a research to determine the application of a carbon paste electrode reformed using 3-(4′-amino-3′-hydroxy-biphenyl-4-yl)-acrylic acid and ZrO_2 nanoparticles which was constructed using a simple and prompt method. The SWV hydrazine peak currents exhibited linear enhancement within 2.5×10^{-8} to 5.0×10^{-5} M hydrazine concentration range and 14 nM detection limit. The sensitivity of 3.992 μA μM^{-1} was obtained for hydrazine.[209]

Mazloum Ardakani reported the application of a CPE reformed using quanizarine (QZ) and TiO_2 nanoparticles. Hydrazine differential pulse voltammetric peak currents exhibited a linear increase within 0.5 to 1900.0 μM concentration limit for hydrazine with 77 nM detection limit. The sensitivity for hydrazine was found to be 0.6022 μA μM^{-1}. The electrode was applied to determine hydrazine within water specimens by utilizing the standard addition method.[210]

Mazloum Ardakani *et al.* applied the CPE reformed using QZ and TiO_2 nanoparticles to determine hydroxylamine. At an optimal state, there was a linear concentration range of 1.0 to 400.0 μM for

Open Access Article. Published on 04 June 2020. Downloaded on 11/7/2025 11:42:49 AM.
This article is licensed under a Creative Commons Attribution-NonCommercial 3.0 Unported Licence.

Table 4 Selected applications of CPEs to environment pollution analysis

Analyte	Modifier	Electrochemical method	Linear range	Detection limit	Ref.
Fomesafen	Carbon nanotube (CNT)	SWV	0.30–40 mg L^{-1}	0.089 mg L^{-1}	182
Methyl parathion	ZrO_2-nanoparticles	SWV	5.0–3000.0 ng mL^{-1}	2.0 ng mL^{-1}	183
Diazinon	Carbon nanotubes (CNTS)	DPV	1×10^{-10} to 6×10^{-8} M	4.5×10^{-10} M	184
Cd(II) Pb(II) Ni(II)	Bismuth nanoparticles	SWASV	1–100 ppb 1–100 ppb 10–150 ppb	0.81 ppb 0.65 ppb 5.47 ppb	192
Cd^{2+} Pb^{2+}	Antimony nanoparticles (SbNPs)/multiwalled carbon nanotubes (MWCNT)	SWASV	10.0–60.0 μg L^{-1}	0.77 μg L^{-1} 0.65 μg L^{-1}	193
Pb^{2+} Cd^{2+} Cu^{2+}	Gold nanoparticles (Au NPs)	SWASV	50–500 μg L^{-1} 200–700 μg L^{-1} 200–700 μg L^{-1}	9.178 μg L^{-1} 86.327 μg L^{-1} 85.373 μg L^{-1}	194
Cd^{2+}	Graphene/TMU-16-NH_2([$Zn_2(NH_2$-BDC$)_2$(4-bpdh)]·3DMF) metal–organic framework (MOF) [graphene/MOF (TMU-16-NH_2)]	DPV	0.7–120 μg L^{-1}	0.2 μg L^{-1}	195
Cu^{2+} Cd^{2+}	Silica nanoparticles/Schiff base ligand (L/SiO_2 NPs)	SWASV	4.0–400.0 ng mL^{-1} 5.0–700.0 ng mL^{-1}	0.28 ng mL^{-1} 0.54 ng mL^{-1}	196
Hg^{2+}	Carbon ionic liquid/ion imprinted polymeric (IIP) nanobeads	DPV	0.5 nM to 2.0 μM	0.1 nM	197
Sn^{2+}	Clinoptilolite nano-particles (CNP)/hexadecyltrimethyl ammonium bromide surfactant (HDTMA)/dithizone (DZ) CNP/HDTMA/DZ	SWV	1×10^{-8} - 1×10^{-2} M	9×10^{-9} M	198
Silver(I)	Poly(methylene disulfide) nanoparticles (PMDSNPs)	DPASV	3.0×10^{-12} to 1.0×10^{-9} M	1.0×10^{-13} M	199
Silver(I)	Magnetic silver ion imprinted polymer nanoparticles (mag-IIP-NPs) Fe_3O_4@SiO_2@IIP	DPV	0.05–150 μg L^{-1}	15 ng L^{-1}	200
Sulfite	Benzoylferrocene (BF)/ionic liquid (n-hexyl-3-methylimidazolium hexafluoro phosphate)/graphene nano-sheets	SWV	5.0×10^{-8} to 2.5×10^{-4} M	20.0 nM	205
Hydrazine	Ionic liquid (2-(4-oxo-3-phenyl-3,4-dihydroquinazolinyl)-*N*′-phenyl hydrazinecarbothioamide)/magnetic core/shell Fe_3O_4@SiO_2/MWCNT nanocomposite	SWV	7.0×10^{-8} to 5.0×10^{-4} M	40.0 nM	206
Sulfite	Ferrocene (FC)/multiwall carbon nanotubes (MWCNTs)	SWV	0.4–120.0 μM	0.1 μM	207
Hydroxylamine	Benzoylferrocene (BF)/carbon nanotubes (CNTs)	SWV	0.9–400.0 μM	0.1 μM	208
Hydrazine	3-(4-Amino-3-hydroxy-biphenyl-4-yl)-acrylic acid/ZrO_2 nanoparticles (ZrO_2 NPs)	SWV	2.5×10^{-8} to 5.0×10^{-5} M	14 nM	209
Hydrazine	TiO_2 nanoparticles/quinizarine (TiO_2 NPs/QZ)	DPV	0.5–1900.0 μM	77 nM	210
Hydroxylamine	TiO_2 nanoparticles/quinizarine (TiO_2 NPs/QZ)	DPV	1.0–400.0 μM	0.173 μM	211
Hydrazine	TiO2 nanoparticles/Mn(III) salen	SWV	3×10^{-8} to 4.0×10^{-4} M	10.0 nM	212
Hydroxylamine	Carbon nanotubes and 2,7-bis(ferrocenyl ethyl) fluoren-9-one (2,7-BF)	SWV	5.0×10^{-8} to 5.0×10^{-4} M	15.0 nM	213
Hydroxylamine	1,1-Bis(phenylacetyl)ferrocenele/NiO/CNTs nanocomposite (1,1-BPF/NiO/CNTs)	SWV	0.5–250.0 μM	0.2 μM	214
Hydroxylamine	CdO nanoparticles (CdO/NPs)	SWV	0.09–650.0 μM	0.06 μM	215
Hydroxylamine	Promazine hydrochloride (PHC)/multiwall carbon nanotube (MWCNT)	DPV	0.17–10.0 mM	1.4 nM	216
Hydroxylamine	8,9-Dihydroxy-7-methyl-12*H*-benzothiazolo[2,3-*b*] quinazolin-12-one -ZnO/CNTs (DMBQ/ZnO NPs/CNTs)	SWV	0.09–350 μM	0.04 μM	217
Hydrazine	ZnO/CNTs nanocomposite/*N*-(4-hydroxyphenyl)-3,5-dinitrobenzamide (ZnO/CNTs/HPDB)	LSV	0.02–550.0 μM	8.0 nM	218
Hydrazine	Gold-copper bimetallic nanoparticles supported on nano P zeolite (Au–Cu/NPZ)	CV	0.01–150 mM	0.04 μM	219
Hydrazine	Silver-doped zeolite L nanoparticles (Ag/L)	CV	10 μM to 4.0 mM	1.5 μM	220
Hydrazine	β-Nickel hydroxide nanoplatelets	Amperometry	1.0–1300.0 μM	0.28 μM	221
Nitrite	Chitosan-functionalized silver nanoparticles/multiwalled carbon nanotube (chit-AgNPs/MWCNT)	Cyclic voltammograms	100 nM to 50 μM	30 nM	222
Paracetamol	SnO_2/SnS nanocomposite	DPV	1.0 to 36.0 μM	0.06 μM	223

Open Access Article. Published on 04 June 2020. Downloaded on 11/7/2025 11:42:49 AM.
This article is licensed under a Creative Commons Attribution-NonCommercial 3.0 Unported Licence.

Table 5 An overview on nanomaterials commonly used in CPEs

Nanomaterial	Features	Ref.
Carbon nanotubes (CNTs)	Good electrical conductivity, high chemical stability, high mechanical strength, high surface area, high ability to mediate electron transfer reactions with electroactive species in solution	122, 126, 141, 142, 148, 149, 151, 167, 168, 170–173, 182, 184, 207, 208, 213 and 216
Graphene	Extremely large specific surface area, good electrical conductivity, high electrocatalytic activity, strong mechanical strength, extremely high thermal conductivity, good biocompatibility, good hydrophilicity and dispersibility in water, high electron mobility at room temperature	139,143,152–154,169,205
CNTs based nanocomposite	Improve the electrical and mechanical properties of the composites by CNTs, possess the properties of individual CNTs, metal-NPs, metal oxide-NPs,… with a synergistic effect, excellent catalytic properties of nanoparticles without losing any of the electronic properties of CNTs	121, 123, 125, 146, 150, 162, 193, 206, 214, 217, 218 and 222
ZnO NPs	Wide band gap (3.37 eV), large excitation binding energy (60 eV), high exciton, biocompatibility, low-cost synthesis, non-toxicity, better electrochemical activities, chemical and photochemical stability, high-electron communication features	124
SiO_2 NPs	Large active surface area and high accumulation efficiency	127 and 196
TiO_2 NPs	Good biocompatibility, high conductivity, low cost, optical transparency	129, 138, 144, 166 and 210–212
ZrO_2 NPs	Thermal stability, biocompatibility, chemical inertness, and affinity for the groups containing oxygen, affinity for phosphate groups, good conductivity	128, 145, 147, 183 and 209
MgO NPs	Good electrical conductivity	159
$ZnFe_2O_4$ NPs	Interesting electronic and magnetic properties, chemical and thermal stability, large specific surface area, low bandgap and high conductivity	164 and 175
CdO NPs	Lower density, higher surface area, and distinct optical property	215
β-Nickel hydroxide nanoplatelets	Relative stability in alkaline medium, the formation of $Ni(OH)_2$/NiOOH redox couple on the electrode surface in alkaline medium, accelerate electron transfer	221
SnO_2	A large band gap of 36 eV, catalytic activity, good compatibility and biocompatibility, non-toxic, inexpensive, green material, good chemical stability and medium conductivity	223
Ni NPs	Enhance electrode conductivity and surface area, facilitate the electron transfer, improve the detection limit of analyte	137
Bi NPs	High surface area	192
Au NPs	Finely tunable optical properties, high surface area, capacity for surface modification, superior stability, complete recovery in biochemical redox processes, less toxic	194
Quantum dot	Very small size, large specific surface area, excellent biocompatibility, quantum cavity electrochemical conductivity	140 and 160
Nanozeolite	High exchange ability, adsorption capacity, increased surface area, decreased diffusion path lengths, presence of more pore entrances per weight amount of zeolite, enhanced diffusion rates and reactivities	198, 219 and 220
Metal–organic framework nanostructure	Extensive porosity, tunable pore sizes, large internal surface area and high degree of crystallinity, good chemical stability in aqueous media and electrochemical oxidation/reduction capability	130 and 195
Y_2O_3 nanoparticles supported on nitrogen-doped reduced graphene oxide (Y_2O_3NPs/N-rGO)	Available nitrogen sources, biocompatible C–N microenvironment, the low production cost, high electrical conductivity and many chemically active sites	158
Reduced graphene oxide/ZnO nanocomposite (rGO/ZnO-NC)	Wide band gap, non-toxicity, large surface area, excellent conductivity and electrocatalytic activity	161
Mesoporous silica nanoparticles (MSNs)	Very high specific surface areas, good adsorption of several species, intrinsic electrocatalytic activity	163
SnO_2–Co_3O_4@rGO nanocomposite	Large electroactive surface area and good electrical conductivity	165
Al_2O_3-supported palladium nanoparticles (PdNPs@Al_2O_3)	High mechanical strength and compressive strength of Al_2O_3-supported	176
Carbon ionic liquid/ion imprinted polymeric nanobeads (IIP-CIL)	High potential and selectivity in trace and ultratrace analyses, high adsorption capacities, improved sensitivity, high stability and durability against harsh chemical environments	197
Poly(methylene disulfide) nanoparticles (PMDSNPs)	The presence of S–S bonds in their main chains, the ability to interact with silver ions	199
Magnetic silver ion imprinted polymer nanoparticles (mag-IIP-NPs) Fe_3O_4@SiO_2@IIP	Simple and convenient to prepare, high selectivity, fast mass transfer, high surface area and good sorption capacity	200

 This journal is © The Royal Society of Chemistry 2020

Open Access Article. Published on 04 June 2020. Downloaded on 11/7/2025 11:42:49 AM. This article is licensed under a Creative Commons Attribution-NonCommercial 3.0 Unported Licence.

hydroxylamine with 0.173 μM LOD *via* the DPV approach. The electrode demonstrated good sensitivity of 0.536 μA μM^{-1}.[211]

Mahmoudi Moghaddam *et al.* fabricated an electrochemical sensor for hydrazine selective and sensitive determination with the existence of phenol. Bulk CPE reformation using TiO_2 nanoparticles and Mn(III) salen. By using the SWV method, 3×10^{-8} to 4.0×10^{-4} M linear dynamic range with 10 nM LOD was determined for hydrazine. A sensitivity of 0.101 μA μM^{-1} was obtained for hydrazine.[212]

Mahmoudi Moghaddam *et al.* examined hydroxylamine electrochemical oxidation at CPE surface which was adjusted using CNTs and 2,7-BF. The electrode's electrochemical reaction properties concerning hydroxylamine and phenol was studied. There was a linear increase regarding SWV hydroxylamine currents at 2,7-BFCNPE within 5.0×10^{-8} to 5.0×10^{-4} M concentration limit and 15 nM LOD for hydroxylamine. The sensitivity of hydroxylamine was found to be 0.319 μA μM^{-1}.[213]

Golestanifar *et al.* examined the electrochemical behavior of hydroxylamine at a 1,1-bis(phenylacetyl)ferrocenele (1,1-BPF)/NiO/CNTs adjusted CPE. There was a linear increase of peak current within the 0.5–250.0 μM concentration range and 0.2 μM LOD for hydroxylamine. The sensitivity was 0.0991 μA μM^{-1}. This sensor was used for wastewater specimens with exceptional results.[214]

Shabani-Nooshabadi and Tahernejad-Javazmi examined the development of a sensitive voltammetric sensor to electrocatalytically determine hydroxylamine with the existence of thiosulfate (TS). When using SWV, hydroxylamine displayed 0.09–650.0 μM linear dynamic range at 0.06 μM detection limit. The sensor exhibited a sensitivity of 0.0589 μA μM^{-1}. This sensor was applied to determine hydroxylamine within water specimens.[215]

Rezaei *et al.* presented an electrochemical sensor to determine hydroxylamine. The developed sensor is supplied with promazine hydrochloride (PHC) which takes the role of a homogenous mediator and MWCNT to enhance the CPE surface as an applicable electrode. Hydroxylamine oxidation electrocatalytic peak current exhibited linear dependency within the 0.008 to 0.100 μM hydroxylamine concentration range *via* DPV at optimal state pH 9. By utilizing LSV under the same circumstances, the calibration plot was achieved within the 0.17 to 10.0 μM concentration range and 1.4 nM LOD for hydroxylamine. Also, sensitivity in the DPV measurement was 476 μA μM^{-1}.[216]

Gupta *et al.* reported the fabrication of a 8,9-dihydroxy-7-methyl-12*H*-benzothiazolo[2,3-*b*]quinazolin-12-one (DMBQ)-ZnO/CNTs adjusted CPE to electro-catalytically ascertain hydroxylamine with the existence of sulfite and phenol within water and waste water specimens. There was a linear increase in terms of SWV peaks within the 0.09–350 μM concentration range and 0.04 μM LOD for hydroxylamine. The sensitivity of the sensor was estimated to be 0.7548 μA μM^{-1}.[217]

Karimi Maleh *et al.*, reported the development of an electrochemical sensor to determine hydrazine with the existence of phenol in water and wastewater specimens. The voltammetric sensor to determine phenol and hydrazine within water and wastewater specimens was an electrode adjusted using ZnO/CNTs nanocomposite and *N*-(4-hydroxyphenyl)-3,5-dinitrobenzamide (HPDB). Hydrazine SWV at the adjusted electrode displayed linear dynamic range of 0.02–550.0 μM and 8.0 nM LOD. The electrochemical sensor showed a sensitivity of 18.4860 μA μM^{-1}.[218]

Amiripour *et al.* described an inexpensive electrochemical sensor on the basis of bimetallic Au–Cu nanoparticles incorporated on P nanozeolite adjusted CPE to determine hydrazine at trace levels. This sensor exhibited beneficial analytical characteristics to determine hydrazine at 0.04 μM detection limit, 0.01–150 mM wide linear range and 99.53 μA mM^{-1} high sensitivity.[219]

Salek Gilani *et al.* proposed a silver loaded nanozeolite adjusted CPE which was utilized as a sensing platform to improve electrocatalytic oxidation and determination of hydrazine. Concerning the amperometric hydrazine determination, a linear range of 10 μM to 4.0 mM was exhibited with 103.13 μA mM^{-1} sensitivity. The LOD of this sensor was determined to be 1.5 μM. The associated reaction time and LOD was 2 seconds and 1.5 μM, correspondingly.[220]

Avanes *et al.* conducted a study on electrocatalytic oxidation and amperometric determination of hydrazine *via* β-nickel hydroxide nanoplatelets altered CPE. This altered electrode exhibited beneficial analytical characteristics to determine hydrazine at 0.28 μM detection limit, 1.0–1300.0 μM wide linear range and 1.33 μA μmol^{-1} L cm^{-2} high sensitivity.[221]

Bibi *et al.* evaluated nitrite voltammetry by utilizing multi-walled carbon nanotube paste electrode (MWCNTPE) adjusted using chitosan-functionalized silver nanoparticles (chit-AgNPs). The oxidation peak current exhibited linear dependency on nitrite concentrations across the 100 nM to 50 μM range and 30 nM nitrite detection limit, correspondingly. The sensitivity (367 881 μA M^{-1}) of sensor was obtained. The developed electrode exhibited high selectivity for nitrite even in the presence of other potentially interfering ions.[222]

A CPE altered using SnO_2/CuS, SnO_2/SnS and Cu@SnO_2/SnS nanocomposites was implemented by Naghian *et al.* to voltammetric sensors for paracetamol (PAT) and hydroquinone (HQ). Within the concentration range of 1.0 to 36 μM for PAT and 1.0 to 85 μM for HQ, linear calibration curves were achieved. The sensitivities are 7.07 μA μM^{-1} cm^{-2} for PAT and 1.8 μA μM^{-1} cm^{-2} for HQ, respectively. The associated detection limits for the analytes were 0.06 μM and 0.2 μM for paracetamol and hydroquinone, correspondingly.[223] Furthermore, the nanoparticle-based electrodes are also intensively studied by previous reports.[224–240]

The uses of CPEs in environmental contamination analysis is surveyed on Table 4. This data outlines the progression and individual trends that were previously mentioned. An overview on nanomaterials commonly used in CPEs listed in Table 5.

Conclusion and future perspectives

CPEs are vital assessment tools to meet the continuously increasing need for prompt, sensitive and selective detection of environmental contaminants, pharmaceutical compounds and biological species. These low-cost electrodes may simply be

Open Access Article. Published on 04 June 2020. Downloaded on 11/7/2025 11:42:49 AM.
This article is licensed under a Creative Commons Attribution-NonCommercial 3.0 Unported Licence.

adapted for the detection of an extensive range of analytes. In this report, original fabrications of CPEs along with their uses in environmental and biological analysis are summarized. There are currently two types of carbon paste design: devices that can be applied for concurrent detection and devices with specificity. The different nanomaterials applied as modifier to alter the working system. The resulting electrodes performed better than to the bare CPE that made them niche and shown potential in the field of electrochemical methods.

Regarding the research area of electroanalysis and environmental contaminants, pharmaceutical compounds, and biological species using nanomaterials-based CPEs, the key interests for the future fundamental research can be summarized as:

(1) More frequent usage of new carbon pastes made of various materials simulating the function of some modifiers (*e.g.*, electrocatalytic properties of carbon nanotubes, functionalized carbon nanotubes, graphene and its derivatives, and ionic liquids) or stabilizing the carbon paste mixture for practical application.

(2) Development a robust synthesis and modification system to prepare nanomaterials with desired properties, *e.g.* highly stable, well-dispersed, highly uniform, and high electrical conductivity to increase the sensitivity and selectivity of electrochemical sensors.

(3) The efficient combination of different nanoscaled materials with each other may open up a new avenue for utilizing novel nanocomposites as the enhancing elements to construct electrochemical sensing platforms (nanocomposite/CPE) with high performance.

(4) Further miniaturization in the field of electrochemical sensing using nanomaterials-based carbon paste electrodes.

(5) Practical preference of methods with favorable ecological parameters (environmentally friendly procedures connected with "green analytical chemistry"). In this respect, nearly harmless and non-toxic carbon pastes can be a considerable advantage.

(6) Combination of traditional electrochemical techniques with other detection methods such as electrochemiluminescence, spectroelectrochemistry, *etc.*

Conflicts of interest

The authors declare that they have no competing interests.

Acknowledgements

This research was supported by China Scholarship Council (201808260042). Furthermore, the financial supports of the Future Material Discovery Program (2016M3D1A1027666) and the Basic Science Research Program (2017R1A2B3009135) through the National Research Foundation of Korea are appreciated.

References

1 V. Gupta, H. Karimi-Maleh, S. Agarwal, F. Karimi, M. Bijad, M. Farsi and S. A. Shahidi, *Sensors*, 2018, **18**, 2817.
2 J. Anojčić, V. Guzsvány, O. Vajdle, Z. Kónya and K. Kalcher, *Monatsh. Chem.*, 2018, **149**, 1727.
3 N. S. Punde, V. G. Kapade and A. K. Srivastava, *J. Electroanal. Chem.*, 2018, **825**, 87.
4 M. U. Anu Prathap, B. Kaur and R. Srivastava, *Chem. Rec.*, 2019, **19**, 883.
5 N. S. Anuar, W. J. Basirun, M. Ladan, M. Shalauddin and M. S. Mehmood, *Sens. Actuators, B*, 2018, **266**, 375.
6 H. Mahmoudi-Moghaddam, S. Tajik and H. Beitollahi, *Food Chem.*, 2019, **286**, 191.
7 Z. Wen, X. Niu, X. Li, W. Zhao, X. Li, D. Ma, D. Dongxue, S. Ying, X. Sun and W. Sun, *Curr. Anal. Chem.*, 2018, **14**, 452.
8 P. R. Oliveira, C. Kalinke, A. S. Mangrich, L. H. Marcolino-Junior and M. F. Bergamini, *Electrochim. Acta*, 2018, **285**, 373.
9 M. Mazloum-Ardakani, H. Beitollahi, M. K. Amini, B.-F. Mirjalili and F. Mirkhalaf, *J. Electroanal. Chem.*, 2011, **651**, 243.
10 L. Fu, A. Wang, G. Lai, C. T. Lin, J. Yu, A. Yu, Z. Liu, K. Xie and W. Su, *Microchim. Acta*, 2019, **186**, 413.
11 P. Talay Pınar, Y. Yardım and Z. Şentürk, *Sens. Actuators, B*, 2018, **273**, 1463.
12 M. A. Khalilzadeh, S. Tajik, H. Beitollahi and R. A. Venditti, *Ind. Eng. Chem. Res.*, 2020, **59**, 4219.
13 Y. Zhang, J. Shen, H. Li, L. Wang, D. Cao, X. Feng, Y. Liu, Y. Ma and L. Wang, *Chem. Rec.*, 2016, **16**, 273.
14 N. A. Abdallah and S. Ahmed, *J. Electrochem. Soc.*, 2018, **165**, H756.
15 B. Norouzi and A. Gorji, *Ionics*, 2019, **25**, 797.
16 R. N. Adams, *Anal. Chem.*, 1958, **30**, 1576.
17 R. Fayazi and M. Ghanei-Motlagh, *Anal. Bioanal. Chem. Res.*, 2019, **6**, 1.
18 T. Kuwana and W. G. French, *Anal. Chem.*, 1964, **36**, 241.
19 G. Li, *J. Appl. Phys.*, 2020, **127**, 010901.
20 B. Cen, K. Li, C. Lv and R. Yang, *J. Solid State Electrochem.*, 2020, **24**, 687.
21 J. Lin, Z. Zhu, C. F. Cheung, F. Yan and G. Li, *J. Mater. Chem. C*, 2020, DOI: 10.1039/d0tc01112f.
22 G. Li, X. Mo, W. C. Law and K. C. Chan, *ACS Appl. Mater. Interfaces*, 2019, **11**, 238.
23 L. Pei, F. Qiu, Y. Ma, F. Lin, C. Fan and X. Ling, *Curr. Pharm. Anal.*, 2020, **16**, 153.
24 A. S. Saad, A. M. A. Al-Alamein, M. M. Galal and H. E. Zaazaa, *J. Electrochem. Soc.*, 2019, **166**, B103.
25 C. M. Kuskur, B. E. Kumara Swamy and H. Jayadevappa, *Ionics*, 2019, **25**, 1845.
26 H. Beitollahi, S. Tajik, M. H. Asadi and P. Biparva, *J. Anal. Sci. Technol.*, 2014, **5**, 29.
27 K. Tiwari, B. Tudu, R. Bandyopadhyay, A. Chatterjee and P. Pramanik, *J. Sens. Sens. Syst.*, 2018, **7**, 319.
28 N. Mouhamed, K. Cheikhou, G. E. Momar Rokhy, D. Moussa Bagha, M. D. Codou Guèye and T. Tzedakis, *Am. J. Anal. Chem.*, 2018, **9**, 171.
29 N. Sohrabi-Gilani, M. H. Nasirtabrizi and A. Parchehbaf Jadid, *Measurement*, 2018, **125**, 84.
30 T. Ören, Ö. Birel and Ü. Anık, *Anal. Lett.*, 2018, **51**, 1680.

 This journal is © The Royal Society of Chemistry 2020

Open Access Article. Published on 04 June 2020. Downloaded on 11/7/2025 11:42:49 AM.
This article is licensed under a Creative Commons Attribution-NonCommercial 3.0 Unported Licence.

31 M. Zhu, H. Ye, M. Lai, J. Ye, J. Kuang, Y. Chen, J. Wang and Q. Mei, *Int. J. Electrochem. Sci.*, 2018, **13**, 4100.
32 Y. Nikodimos, B. Hagos, D. Dereje and M. Hussen, *Chem. Int.*, 2018, **4**, 43.
33 N. A. Abdallah and S. Ahmed, *J. Electrochem. Soc.*, 2018, **165**, H756.
34 N. P. Shetti, S. Deepti Nayak, J. Shweta Malode and M. Raviraj Kulkarni, *Carbon*, 2018, **8**, 10.
35 M. R. Akanda, M. Sohail, M. A. Aziz and A. N. Kawde, *Electroanalysis*, 2016, **28**, 408.
36 S. Tajik, M. A. Taher, H. Beitollahi and M. Torkzadeh-Mahani, *Talanta*, 2015, **134**, 60.
37 S. Sharifian and A. Nezamzadeh-Ejhieh, *Mater. Sci. Eng., C*, 2016, **58**, 510.
38 L. Tian, Y. Gao, L. Li, W. Wu, D. Sun, J. Lu and T. Li, *Microchim. Acta*, 2013, **180**, 607.
39 A. Benvidi, M. T. Nafar, S. Jahanbani, M. D. Tezerjani, M. Rezaeinasab and S. Dalirnasab, *Mater. Sci. Eng., C*, 2017, **75**, 1435.
40 M. Akhoundian, T. Alizadeh, M. R. Ganjali and P. Norouzi, *Talanta*, 2019, **200**, 115.
41 M. Shehata, S. M. Azab, A. M. Fekry and M. A. Ameer, *Biosens. Bioelectron.*, 2016, **79**, 589.
42 Z. Stanić and S. Girousi, *Sensing in electroanalysis*, 2011, vol. 6, p. 89.
43 K. Vytřas, I. Švancara and R. Metelka, *J. Serb. Chem. Soc.*, 2009, **74**, 1021.
44 J. Munoz and M. Baeza, *Electroanalysis*, 2017, **29**, 1660.
45 I. Svancara, K. Kalcher, A. Walcarius and K. Vytras, *Electroanalysis with carbon paste electrodes*, CRC Press, Taylor & Francis Group, Boca Raton, Florida, United States, 2012.
46 S. A. Zaidi, *Int. J. Electrochem. Sci.*, 2013, **8**, 11337.
47 E. Nossol and A. J. Zarbin, *Electrochim. Acta*, 2008, **54**, 582.
48 R. N. Adams, *Electrochemistry at Solid Electrodes*, Dekker, New York, 1969, p. 280.
49 P. Tuzhi, L. Huiping and W. Shuwen, *Analyst*, 1993, **118**, 1321.
50 J. Pei, Q. Yin and J. Zhong, *Talanta*, 1991, **38**, 1185.
51 K. Pliuta, A. Chebotarev, A. Koicheva, K. Bevziuk and D. Snigur, *Anal. Methods*, 2018, **10**, 1472.
52 M. Mahanthappa, N. Kottam and S. Yellappa, *Anal. Methods*, 2018, **10**, 1362.
53 G. K. Jayaprakash, B. E. Kumara Swamy, H. N. González Ramírez, M. T. Ekanthappa and R. Flores-Moreno, *New J. Chem.*, 2018, **42**, 4501.
54 S. K. Hassaninejad-Darzi and F. Shajie, *Mater. Sci. Eng., C*, 2018, **91**, 64.
55 L. Xu, S. Xie, J. Du and N. He, *J. Nanosci. Nanotechnol.*, 2017, **17**, 238.
56 M. Ghaedi, S. Y. Shajaripour Jaberi, S. Hajati, M. Montazerozohori, M. Zarr, A. Asfaram, L. K. Kumawat and V. K. Gupta, *Electroanalysis*, 2015, **27**, 1516.
57 P. K. Kalambate and A. K. Srivastava, *Sens. Actuators, B*, 2016, **233**, 237.
58 A. Afkhami, H. Khoshsafar, H. Bagheri and T. Madrakian, *Sens. Actuators, B*, 2014, **203**, 909.
59 H. Karimi-Maleh, A. L. Sanati, V. K. Gupta, M. Yoosefian, M. Asif and A. Bahari, *Sens. Actuators, B*, 2014, **204**, 647.
60 V. Arabali, M. Ebrahimi, S. Gheibi, F. Khaleghi, M. Bijad, A. Rudbaraki, M. Abbasghorbani and M. R. Ganjali, *Food Anal. Methods*, 2016, **9**, 1763.
61 M. Bijad, H. Karimi-Maleh, M. Farsi and S. A. Shahidi, *Food Anal. Methods*, 2017, **10**, 3773.
62 V. Gautam, P. S. Karan and L. Y. Vijay, *Anal. Bioanal. Chem.*, 2018, **410**, 2173.
63 V. Gautam, K. Pratap Singh and V. Laxmi Yadav, *Int. J. Biol. Macromol.*, 2018, **111**, 1124.
64 N. Soltani, N. Tavakkoli, Z. S. Mosavimanesh, F. Davar and C. R. Chim, *Can. J. Chem.*, 2018, **21**, 54.
65 A. A. Rafati, A. Afraz, A. Hajian and P. Assari, *Microchim. Acta*, 2014, **181**, 1999.
66 Z. Amani-Beni and A. Nezamzadeh-Ejhieh, *New J. Chem.*, 2018, **42**, 1021.
67 E. Y. Frag, N. A. Abd El-Ghany and M. A. E. L. Fattah, *J. Electroanal. Chem.*, 2018, **808**, 266.
68 A. M. Hassanein, Y. I. Moharram, N. F. Oraiby and S. E. Ebied, *Am. J. Anal. Chem.*, 2017, **8**, 708.
69 Y. Liu, K. Liu, H. Dong, L. Zhang, Y. Deng, C. Ma and Z. Wang, *Nanosci. Nanotechnol. Lett.*, 2016, **8**, 785.
70 N. Nontawong, M. Amatatongchai, S. Thimoonnee, S. Laosing, P. Jarujamrus, C. Karuwan and S. Chairam, *J. Pharm. Biomed. Anal.*, 2019, **175**, 112770.
71 M. Torkashvand, M. Bagher Gholivand, A. Arman Taherpour, A. Boochani and A. Akhtar, *J. Pharm. Biomed. Anal.*, 2017, **139**, 156.
72 N. Xiao, J. Deng, J. Cheng, S. Ju, H. Zhao, J. Xie, D. Qian and J. He, *Biosens. Bioelectron.*, 2016, **81**, 54.
73 M. B. Gholivand and M. Torkashvand, *Mater. Sci. Eng., C*, 2015, **48**, 235.
74 P. R. de Oliveira, A. C. Lamy-Mendes, J. L. Gogola, A. S. Mangrich, L. H. Marcolino Junior and M. F. Bergamini, *Electrochim. Acta*, 2015, **151**, 525.
75 S. Yang, G. Li, G. Wang, J. Zhao, Z. Qiao and L. Qu, *Sens. Actuators, B*, 2015, **206**, 126.
76 M. Shabani-Nooshabadi, M. Roostaee and F. Tahernejad-Javazmi, *J. Mol. Liq.*, 2016, **219**, 142.
77 S. Cheraghi, M. A. Taher and H. Fazelirad, *Microchim. Acta*, 2013, **180**, 1157.
78 T. M. B. F. Oliveira, M. Fátima Barroso, S. Morais, M. Araújo, C. Freire, P. de Lima-Neto, A. N. Correia, M. B. P. P. Oliveira and C. Delerue-Matos, *Bioelectrochemistry*, 2014, **98**, 20.
79 X. Wang, Z. You, H. Sha, S. Gong, Q. Niu and W. Sun, *Microchim. Acta*, 2014, **181**, 767.
80 S. D. Bukkitgar and N. P. Shetti, *Mater. Sci. Eng., C*, 2016, **65**, 262.
81 P. K. Kalambate, C. R. Rawool and A. K. Srivastava, *Sens. Actuators, B*, 2016, **237**, 196.
82 M. Khadem, F. Faridbod, P. Norouzi, A. Rahimi Foroushani, M. R. Ganjali, S. J. Shahtaheri and R. Yarahmadi, *Electroanalysis*, 2017, **29**, 708.
83 P. K. Kalambate, C. R. Rawool, S. P. Karna and A. K. Srivastava, *Mater. Sci. Eng., C*, 2016, **69**, 453.

Open Access Article. Published on 04 June 2020. Downloaded on 11/7/2025 11:42:49 AM.
This article is licensed under a Creative Commons Attribution-NonCommercial 3.0 Unported Licence.

84 F. Karimi, A. Fallah Shojaei, K. Tabatabaeian and Sh. Shakeri, *J. Mol. Liq.*, 2017, **242**, 685.
85 H. Ibrahim and Y. Temerk, *Sens. Actuators, B*, 2015, **206**, 744.
86 Y. Tepeli, B. Demir, S. Timur and U. Anik, *RSC Adv.*, 2015, **5**, 53973.
87 K. J. Huang, J. Y. Sun, C. X. Xu, D. J. Niu and W. Z. Xie, *Microchim. Acta*, 2010, **168**, 51.
88 J. Peng, Y. Feng, X. X. Han and Z. N. Gao, *Microchim. Acta*, 2016, **183**, 2289.
89 Z. Amani-Beni and A. Nezamzadeh-Ejhieh, *J. Colloid Interface Sci.*, 2017, **504**, 186.
90 L. Ahmadpour-Mobarakeh and A. Nezamzadeh-Ejhieh, *Mater. Sci. Eng., C*, 2015, **49**, 493.
91 T. Alizadeh, M. R. Ganjali and F. Rafiei, *Anal. Chim. Acta*, 2017, **974**, 54.
92 M. Amatatongchai, W. Sroysee, S. Chairam and D. Nacapricha, *Talanta*, 2017, **166**, 420.
93 Y. E. L. Bouabi, A. Farahi, N. Labjar, S. El Hajjaji, M. Bakasse and M. A. El Mhammedi, *Mater. Sci. Eng., C*, 2016, **58**, 70.
94 M. Saadat and A. Nezamzadeh-Ejhieh, *Electrochim. Acta*, 2016, **217**, 163.
95 S. Liu and H. Ju, *Biosens. Bioelectron.*, 2003, **19**, 177.
96 H. Liu, P. He, Z. Li, C. Sun, L. Shi, Y. Liu, G. Zhu and J. Li, *Electrochem. Commun.*, 2005, **7**, 1357.
97 Y. Zhang, G. M. Zeng, L. Tang, D. L. Huang, X. Y. Jiang and Y. N. Chen, *Biosens. Bioelectron.*, 2007, **22**, 2121.
98 M. Elyasi, M. A. Khalilzadeh and H. Karimi-Maleh, *Food Chem.*, 2013, **141**, 4311.
99 S. Wei, W. Dandan, G. Ruifang and J. Kui, *Electrochem. Commun.*, 2007, **9**, 1159.
100 W. Sun, R. Gao and K. Jiao, *J. Phys. Chem. B*, 2007, **111**, 4560.
101 Y. Lin, X. Cui and L. Li, *Electrochem. Commun.*, 2005, **7**, 166.
102 R. Ojani, J. B. Raoof and S. R. H. Zavvarmahalleh, *Electrochim. Acta*, 2008, **53**, 2402.
103 H. Yin, Y. Zhou and S. Ai, *J. Electroanal. Chem.*, 2009, **626**, 80.
104 Y. Zhang and J. B. Zheng, *Electrochim. Acta*, 2007, **52**, 7210.
105 M. A. El Mhammedi, M. Achak, M. Bakasse and A. Chtaini, *J. Hazard. Mater.*, 2009, **163**, 323.
106 P. Mulchandani, M. C. Hangarter, Y. Lei, W. Chen and A. Mulchandani, *Biosens. Bioelectron.*, 2005, **21**, 523.
107 T. Alizadeh, M. R. Ganjali, P. Norouzi, M. Zare and A. Zeraatkar, *Talanta*, 2009, **79**, 1197.
108 G. Aragay, J. Pons and A. Merkoçi, *Chem. Rev.*, 2011, **111**, 3433.
109 A. Düzgün, G. A. Zelada-Guillén, G. A. Crespo, S. Macho, J. Riu and F. X. Rius, *Anal. Bioanal. Chem.*, 2011, **399**, 171.
110 L. Wang, W. Ma, L. Xu, W. Chen, Y. Zhu, C. Xu and N. A. Kotov, *Mater. Sci. Eng., R*, 2010, **70**, 265.
111 A. Chen and S. Chatterjee, *Chem. Soc. Rev.*, 2013, **42**, 5425.
112 Y. Zeng, Z. Zhu, D. Du and Y. Lin, *J. Electroanal. Chem.*, 2016, **781**, 147.
113 C. S. Padidem, S. Bashir and J. Liu, Sensor enhancement using nanomaterials to detect pharmaceutical residue: nanointegration using phenol as environmental pollutant, in *New Perspectives in Biosensors Technology and Applications*, ed. P.A. Serra, Italy, 2011, pp. 421–448.
114 B. de Falco, A. Fiore, R. Bochicchio, M. Amato and V. Lanzotti, *Ind. Crops Prod.*, 2018, **112**, 584.
115 M. Narasimhaiah, A. Arunachalam, S. Sellappan, V. K. Mayasula, P. R. Guvvala, S. K. Ghosh, V. Chandra, J. Ghosh and H. Kumar, *Reprod. Domest. Anim.*, 2018, **53**, 644.
116 K. R. Avalos-Llano, O. Martín-Belloso and R. Soliva-Fortuny, *Food Chem.*, 2018, **264**, 393.
117 S. Yuan, Z. Duan, Y. Lu, X. Ma and S. Wang, *Biotech*, 2018, **8**, 8.
118 D. Vione, D. Fabbri, M. Minella and S. Canonica, *Water Res.*, 2018, **128**, 38.
119 D. Marín, A. Alemán, A. Sánchez-Faure, P. Montero and M. C. Gómez-Guillén, *Food Chem.*, 2018, **245**, 525.
120 T. Beta and T. Hwang, *Food Chem.*, 2018, **246**, 58.
121 H. Karimi-Maleh, F. Tahernejad-Javazmi, A. A. Ensafi, R. Moradi, S. Mallakpour and H. Beitollahi, *Biosens. Bioelectron.*, 2014, **60**, 1.
122 B. Rezaei, H. Khosropour, A. A. Ensafi, H. Hadadzadeh and H. Farrokhpour, *IEEE Sens. J.*, 2015, **15**, 483.
123 F. Tahernejad-Javazmi, M. Shabani-Nooshabadi and H. Karimi-Maleh, *Talanta*, 2018, **176**, 208.
124 H. Beitollahi, A. Gholami and M. R. Ganjali, *Mater. Sci. Eng., C*, 2015, **57**, 107.
125 M. Roodbari-Shahmiri, A. Bahari, H. Karimi-Maleh, R. Hosseinzadeh and N. Mirnia, *Sens. Actuators, B*, 2013, **177**, 70.
126 A. Abellán-Llobregat, C. González-Gaitán, L. Vidal, A. Canals and E. Morallon, *Biosens. Bioelectron.*, 2018, **109**, 123.
127 J. Tashkhourian and S. F. Nami-Ana, *Mater. Sci. Eng., C*, 2015, **52**, 103.
128 S. A. Shahamirifard, M. Ghaedi, Z. Razmi and S. Hajati, *Biosens. Bioelectron.*, 2018, **114**, 30.
129 J. Tashkhourian, S. F. Nami Ana, S. Hashemnia and M. R. Hormozi-Nezhad, *J. Solid State Electrochem.*, 2013, **17**, 157.
130 H. Valizadeh, J. Tashkhourian and A. Abbaspour, *Microchim. Acta*, 2019, **186**, 455.
131 L. Sominsky, L. Kooi Ong, I. Ziko, P. W. Dickson and S. J. Spencer, *Mol. Cell. Endocrinol.*, 2018, **470**, 295.
132 D. Askri, S. Ouni, S. Galai, B. Chovelon, J. Arnaud, S. G. Lehmann, M. Sakly, M. Sève and S. Amara, *J. Trace Elem. Med. Biol.*, 2018, **50**, 73.
133 D. Piston and M. E. Gegg, *Neural Regener. Res.*, 2018, **13**, 815.
134 S. Ritter, *Appetite*, 2018, **126**, 210.
135 M. Shin, J. H. Ryu, K. Kim, M. J. Kim, S. Jo, M. S. Lee, D. Y. Lee and H. Lee, *ACS Biomater. Sci. Eng.*, 2018, **4**, 2314.
136 J. B. Dai, Y. Chen and J. T. Sakata, *Neuroscience*, 2018, **379**, 415.
137 R. Ojani, S. Gholitabar Omrani, J. B. Raoof and S. Zamani, *Anal. Methods*, 2016, **8**, 2471.

Open Access Article. Published on 04 June 2020. Downloaded on 11/7/2025 11:42:49 AM.
This article is licensed under a Creative Commons Attribution-NonCommercial 3.0 Unported Licence.

138 M. Mazloum-Ardakani, H. Rajabi, H. Beitollahi, B. B. F. Mirjalili, A. Akbari and N. Taghavinia, *Int. J. Electrochem. Sci.*, 2010, **5**, 147.
139 F. Ye, C. Feng, N. Fu, H. Wu, J. Jiang and S. Han, *Appl. Surf. Sci.*, 2015, **357**, 1251.
140 H. Beitollahi, M. Hamzavi, M. Torkzadeh-Mahani, M. Shanesaz and H. Karimi-Maleh, *Electroanalysis*, 2015, **27**, 524.
141 H. Beitollahi and I. Sheikhshoaie, *Anal. Methods*, 2011, **3**, 1810.
142 T. Tavana, M. A. Khalilzadeh, H. Karimi-Maleh, A. A. Ensafi, H. Beitollahi and D. Zareyee, *J. Mol. Liq.*, 2012, **168**, 69.
143 M. D. Tezerjani, A. Benvidi, A. D. Firouzabadi, M. Mazloum-Ardakani and A. Akbari, *Measurement*, 2017, **101**, 183.
144 M. Mazloum-Ardakani, H. Beitollahi, M. A. Sheikh-Mohseni, A. Benvidi, H. Naeimi, M. Nejati-Barzoki and N. Taghavinia, *Colloids Surf., B*, 2010, **76**, 82.
145 M. Mazloum-Ardakani, H. Beitollahi, M. K. Amini, F. Mirkhalaf and M. Abdollahi-Alibeik, *Anal. Methods*, 2011, **3**, 673.
146 A. Pahlavan, V. K. Gupta, A. L. Sanati, F. Karimi, M. Yoosefian and M. Ghadami, *Electrochim. Acta*, 2014, **123**, 456.
147 M. Mazloum-Ardakani, H. Beitollahi, M. K. Amini, F. Mirkhalaf and M. Abdollahi-Alibeik, *Sens. Actuators, B*, 2010, **151**, 243.
148 H. Mahmoudi-Moghaddam and H. Beitollahi, *Int. J. Electrochem. Sci.*, 2011, **6**, 6503.
149 M. Mazloum-Ardakani, H. Beitollahi, B. Ganjipour and H. Naeimi, *Int. J. Electrochem. Sci.*, 2010, **5**, 531.
150 A. Afkhami, F. Kafrashi and T. Madrakian, *Ionics*, 2015, **21**, 2937.
151 H. Beitollahi, J. B. Raoof and R. Hosseinzadeh, *Electroanalysis*, 2011, **23**, 1934.
152 S. Tajik, M. A. Taher and H. Beitollahi, *Electroanalysis*, 2014, **26**, 796.
153 A. M. Santos, A. Wong, F. C. Vicentini and O. Fatibello-Filho, *Microchim. Acta*, 2019, **186**, 174.
154 K. Movlaee, H. Beitollahi, M. R. Ganjali and P. Norouzi, *Microchim. Acta*, 2017, **184**, 3281.
155 H. Kato, A. Kimberly Volterman, D. W. D. West, K. Suzuki and D. R. Moore, *Amino Acids*, 2018, **50**, 1679.
156 Y. Kitajima, H. Takahashi, T. Akiyama, K. Murayama, S. Iwane, T. Kuwashiro and K. Tanaka, *J. Gastroenterol.*, 2018, **53**, 427.
157 J. A. Hutchings, M. R. Shields, T. S. Bianchi and E. A. G. Schuur, *Org. Geochem.*, 2018, **115**, 46.
158 S. Yang, G. Li, Y. Wang, G. Wang and L. Qu, *Microchim. Acta*, 2016, **183**, 1351.
159 V. K. Gupta, Z. Shamsadin-Azad, S. Cheraghi, S. Agarwai, M. A. Taher and F. Karimi, *Int. J. Electrochem. Sci.*, 2018, **13**, 4309.
160 S. Hooshmand and Z. Es'haghi, *J. Pharm. Biomed. Anal.*, 2017, **146**, 226.
161 Z. Karami and I. Sheikhshoaie, *Anal. Bioanal. Electrochem.*, 2017, **9**, 834.
162 Z. Wei, Y. Sun, Q. Yin, L. Wang, S. Chen, R. Sheng, D. Pan, H. Yang and S. Li, *Int. J. Electrochem. Sci.*, 2018, **13**, 7478.
163 S. Karimi and M. Heydari, *Sens. Actuators, B*, 2018, **257**, 1134.
164 S. M. Ghoreishi and M. Malekian, *J. Electroanal. Chem.*, 2017, **805**, 1.
165 H. Zeinali, H. Bagheri, Z. Monsef-Khoshhesab, H. Khoshsafar and A. Hajian, *Mater. Sci. Eng., C*, 2017, **71**, 386.
166 M. Mazloum-Ardakani, H. Beitollahi, Z. Taleat, H. Naeimi and N. Taghavinia, *J. Electroanal. Chem.*, 2010, **644**, 1.
167 A. A. Ensafi and H. Karimi-Maleh, *Drug Test. Anal.*, 2011, **3**, 325.
168 H. Beitollahi, A. Mohadesi, S. Mohammadi and A. Akbari, *Electrochim. Acta*, 2012, **68**, 220.
169 S. Tajik, M. A. Taher and H. Beitollahi, *Sens. Actuators, B*, 2014, **197**, 228.
170 A. A. Ensafi and H. Karimi-Maleh, *Int. J. Electrochem. Sci.*, 2010, **5**, 1484.
171 H. Beitollahi, J. B. Raoof, H. Karimi-Maleh and R. Hosseinzadeh, *J. Solid State Electrochem.*, 2012, **16**, 1701.
172 H. Karimi-Maleh, M. A. Khalilzadeh, Z. Ranjbarha, H. Beitollahi, A. A. Ensafi and D. Zareyee, *Anal. Methods*, 2012, **4**, 2088.
173 S. Tajik, M. A. Taher and H. Beitollahi, *J. Electroanal. Chem.*, 2013, **704**, 137.
174 T. Alizadeh, F. Atashi, M. Akhoundian and M. R. Ganjali, *Microchim. Acta*, 2019, **186**, 654.
175 N. Tavakkoli, N. Soltani, F. Shahdost-fard, M. Ramezani, H. Salavati and M. R. Jalali, *Microchim. Acta*, 2018, **185**, 479.
176 N. Soltani, N. Tavakkoli, F. Shahdost-fard, H. Salavati and F. Abdoli, *Microchim. Acta*, 2019, **186**, 540.
177 J. B. Weber, Properties and behavior of pesticides in soil, in *Mechanisms of pesticide movement into ground water*, CRC Press, Taylor & Francis Group, Boca Raton, Florida, United States, 2018, pp. 15–42.
178 L. Qiu, P. Lv, C. Zhao, X. Feng, G. Fang, J. Liu and S. Wang, *Sens. Actuators, B*, 2019, **286**, 386.
179 F. Smedes, *Chemosphere*, 2018, **210**, 662.
180 M. Tankiewicz and M. Biziuk, *Anal. Bioanal. Chem.*, 2018, **410**, 1533.
181 K. M. Major, D. P. Weston, M. J. Lydy, G. A. Wellborn and H. C. Poynton, *Evol. Appl.*, 2018, **11**, 748.
182 E. Demir and R. İnam, *Food Anal. Methods*, 2017, **10**, 74.
183 H. Parham and N. Rahbar, *J. Hazard. Mater.*, 2010, **177**, 1077.
184 M. Rahimnejad, R. A. Abdulkareem and G. Najafpour, *Biocatal. Agric. Biotechnol.*, 2019, **20**, 101245.
185 Y. Nuapia, L. Chimuka and E. Cukrowska, *Chemosphere*, 2018, **196**, 339.
186 L. Fang, L. Li, Z. Qu, H. Xu, J. Xu and N. Yan, *J. Hazard. Mater.*, 2018, **342**, 617.
187 J. Tang, J. He, X. Xin, H. Hu and T. Liu, *Chem. Eng. J.*, 2018, **334**, 2579.
188 V. Karri, V. Kumar, D. Ramos, E. Oliveira and M. Schuhmacher, *Biol. Trace Elem. Res.*, 2018, **184**, 226.

Open Access Article. Published on 04 June 2020. Downloaded on 11/7/2025 11:42:49 AM.
This article is licensed under a Creative Commons Attribution-NonCommercial 3.0 Unported Licence.

189 T. Wang, H. Sun, X. Ren, B. Li and H. Mao, *Ecotoxicol. Environ. Saf.*, 2018, **148**, 285.
190 T. C. Nguyen, P. Loganathan, T. Vinh Nguyen, J. Kandasamy, R. Naidu and S. Vigneswaran, *Environ. Sci. Pollut. Res.*, 2018, **25**, 20430.
191 J. Wen, Z. Li, N. Luo, M. Huang, R. Yang and G. Zeng, *Ecotoxicol. Environ. Saf.*, 2018, **162**, 184.
192 P. Niu, C. Fernández-Sánchez, M. Gich, C. Ayora and A. Roig, *Electrochim. Acta*, 2015, **165**, 155.
193 A. M. Ashrafi, S. Cerovac, S. Mudrić, V. Guzsvány, L. Husáková, I. Urbanová and K. Vytřas, *Sens. Actuators, B*, 2014, **191**, 320.
194 H. Devnani and S. P. Satsangee, *Int. J. Environ. Sci. Technol.*, 2015, **12**, 1269.
195 M. Roushani, A. Valipour and Z. Saedi, *Sens. Actuators, B*, 2016, **233**, 419.
196 A. Afkhami, M. Soltani-Shahrivar, H. Ghaedi and T. Madrakian, *Electroanalysis*, 2016, **28**, 296.
197 A. Bahrami, A. Besharati-Seidani, A. Abbaspour and M. Shamsipur, *Mater. Sci. Eng., C*, 2015, **48**, 205.
198 A. Niknezhadi and A. Nezamzadeh-Ejhieh, *J. Colloid Interface Sci.*, 2017, **501**, 321.
199 S. M. Ghalebi, V. Zare-Shahabadi and H. Parham, *Microchim. Acta*, 2019, **186**, 60.
200 M. Ghanei-Motlagh and M. A. Taher, *Microchim. Acta*, 2017, **184**, 1691.
201 Z. Li, M. Ren, L. Wang and W. Lin, *Anal. Methods*, 2018, **10**, 4016.
202 B. Hu, X. L. Tian, W. N. Shi, J. Q. Zhao, P. Wu and S. T. Mei, *Int. J. Environ. Sci. Technol.*, 2018, **15**, 323.
203 L. Sparlinek, V. Leitner and B. Kamm, *J. Biotechnol.*, 2018, **284**, 63.
204 M. Wang, W. Wang, M. Ji and X. Cheng, *Appl. Surf. Sci.*, 2018, **439**, 350.
205 H. Beitollahi, S. Tajik and P. Biparva, *Measurement*, 2014, **56**, 170.
206 H. Beitollahi, S. Tajik and Sh. Jahani, *Electroanalysis*, 2016, **28**, 1093.
207 H. Karimi-Maleh, A. A. Ensafi, H. Beitollahi, V. Nasiri, M. A. Khalilzadeh and P. Biparva, *Ionics*, 2012, **18**, 687.
208 M. M. Foroughi, H. Beitollahi, S. Tajik, M. Hamzavi and H. Parvan, *Int. J. Electrochem. Sci.*, 2014, **9**, 2955.
209 S. Z. Mohammadi, H. Beitollahi and E. Bani-Asadi, *Environ. Monit. Assess.*, 2015, **187**, 122.
210 M. Mazloum-Ardakani, H. Beitollahi, Z. Taleat and H. Naeimi, *Anal. Methods*, 2010, **2**, 1764.
211 M. Mazloum-Ardakani, Z. Taleat, H. Beitollahi and H. Naeimi, *Nanoscale*, 2011, **3**, 1683.
212 H. Mahmoudi-Moghaddam, H. Beitollahi, S. Tajik, I. Sheikhshoaie and P. Biparva, *Environ. Monit. Assess.*, 2015, **187**, 407.
213 H. Mahmoudi-Moghaddam, H. Beitollahi, S. Tajik, M. Malakootian and H. Karimi-Maleh, *Environ. Monit. Assess.*, 2014, **186**, 7431.
214 F. Golestanifar, H. Karimi-Maleh, N. Atar, E. Aydoğdu, B. Ertan, M. Taghavi, M. Lütfi Yola and M. Ghaemy, *Int. J. Electrochem. Sci.*, 2015, **10**, 5456.
215 M. Shabani-Nooshabadi and F. Tahernejad-Javazmi, *Electroanalysis*, 2015, **27**, 1733.
216 B. Rezaei, A. A. Ensafi and E. Jamshidi-Mofrad, *Sens. Actuators, B*, 2015, **211**, 138.
217 V. K. Gupta, H. Karimi-Maleh and R. Sadegh, *Int. J. Electrochem. Sci.*, 2015, **10**, 303.
218 H. Karimi-Maleh, M. Moazampour, A. A. Ensafi, S. Mallakpour and M. Hatami, *Environ. Sci. Pollut. Res.*, 2014, **21**, 5879.
219 F. Amiripour, S. N. Azizi and Sh. Ghasemi, *Biosens. Bioelectron.*, 2018, **107**, 111.
220 N. Salek Gilani, S. N. Azizi and S. Ghasemi, *Bull. Mater. Sci.*, 2017, **40**, 177.
221 A. Avanes, M. Hasanzadeh-Karamjavan and G. Shokri-Jarcheloo, *Microchim. Acta*, 2019, **186**, 441.
222 S. Bibi, M. I. Zaman, A. Niaz, A. Rahim, M. Nawaz and M. B. Arian, *Microchim. Acta*, 2019, **186**, 595.
223 E. Naghian and M. Najafi, *Microchim. Acta*, 2018, **185**, 406.
224 K. Zhang, R. S. Varma, H. W. Jang, J. W. Choi and M. Shokouhimehr, *J. Alloys Compd.*, 2019, **791**, 911.
225 K. Zhang, T. H. Lee, B. Bubach, M. Ostadhassan, H. W. Jang, J.-W. Choi and M. Shokouhimehr, *RSC Adv.*, 2019, **9**, 21363.
226 K. Zhang, T. H. Lee, H. Noh, T. Islamoglu, O. K. Farha, H. W. Jang, J.-W. Choi and M. Shokouhimehr, *ACS Appl. Mater. Interfaces*, 2019, **11**, 31799.
227 K. Zhang, K. Hong, J. M. Suh, T. H. Lee, O. Kwon, M. Shokouhimehr and H. W. Jang, *Res. Chem. Intermed.*, 2019, **45**, 599.
228 K. Zhang, J. M. Suh, T. H. Lee, J. H. Cha, J.-W. Choi, H. W. Jang, R. S. Varma and M. Shokouhimehr, *Nano Convergence*, 2019, **6**, 6.
229 K. Zhang, T. H. Lee, B. Bubach, H. W. Jang, M. Ostadhassan, J.-W. Choi and M. Shokouhimehr, *RSC Adv.*, 2019, **9**, 26668.
230 K. Zhang, T. H. Lee, B. Bubach, H. W. Jang, M. Ostadhassan, J.-W. Choi and M. Shokouhimehr, *Sci. Rep.*, 2019, **9**, 13665.
231 K. Zhang, T. H. Lee, J. H. Cha, R. S. Varma, J.-W. Choi, H. W. Jang and M. Shokouhimehr, *Sci. Rep.*, 2019, **9**, 13573.
232 K. Zhang, T. H. Lee, J. H. Cha, H. W. Jang, J.-W. Choi, M. Mahmoudi and M. Shokouhimehr, *Sci. Rep.*, 2019, **9**, 13739.
233 K. Zhang, T. H. Lee, J. H. Cha, H. W. Jang, J.-W. Choi, R. S. Varma and M. Shokouhimehr, *ACS Omega*, 2019, **4**, 21410.
234 K. Zhang, T. H. Lee, O. K. Farha, H. W. Jang, J.-W. Choi and M. Shokouhimehr, *Cryst. Growth Des.*, 2019, **19**, 7385.
235 K. Zhang, T. H. Lee, M. A. Khalilzadeh, R. S. Varma, J.-W. Choi, H. W. Jang and M. Shokouhimehr, *ACS Omega*, 2020, **5**, 1634.
236 H. Beitollahi, M. A. Khalilzadeh, S. Tajik, M. Safaei, K. Zhang, H. W. Jang and M. Shokouhimehr, *ACS Omega*, 2020, **5**, 2049.
237 K. Hong, M. Sajjadi, J. M. Suh, K. Zhang, M. Nasrollahzadeh, H. W. Jang, R. S. Varma and M. Shokouhimehr, *ACS Appl. Nano Mater.*, 2020, **3**, 2070.

 This journal is © The Royal Society of Chemistry 2020

Open Access Article. Published on 04 June 2020. Downloaded on 11/7/2025 11:42:49 AM.
This article is licensed under a Creative Commons Attribution-NonCommercial 3.0 Unported Licence.

238 H. Alamgholiloo, S. Rostamnia, K. Zhang, T. H. Lee, Y.-S. Lee, R. S. Varma, H. W. Jang and M. Shokouhimehr, *ACS Omega*, 2020, **5**, 5182.
239 K. Zhang, T. H. Lee, M. J. Choi, A. Rajabi Abhari, S. Choi, K. S. Choi, R. S. Varma, J. W. Choi, H. W. Jang and M. Shokouhimehr, *Nano Convergence*, 2020, **7**, 1.
240 S. Tajik, H. Beitollahi, M. R. Aflatoonian, B. Aflatoonian, I. Sheikh Shoaie, M. A. Khalilzadeh, K. Zhang, Q. V. Le, H. W. Jang and M. Shokouhimehr, *Microchem. J.*, 2020, **157**, 104890.